Research Square

Preprints are preliminary reports that have not undergone peer review.
They should not be considered conclusive, used to inform clinical practice,
or referenced by the media as validated information.

Comparative transcriptomic and hormonal analyses reveal potential regulation networks of adventitious root formation in Metasequoia glyptostroboides Hu et Cheng

Yuping Xiong
the Chinese Academy of Sciences
Xiaohong Chen
the Chinese Academy of Sciences
Junyu Liu
the Chinese Academy of Sciences
Yuan Li
the Chinese Academy of Sciences
Zhan Bian
the Chinese Academy of Sciences
Xinhua Zhang
the Chinese Academy of Sciences
Songjun Zeng
the Chinese Academy of Sciences
Jaime A. Teixeira da Silva
kagawa ken
Jianrong Li
the Chinese Academy of Sciences
Guohua Ma
magh@scib.ac.cn

the Chinese Academy of Sciences

Research Article

Keywords: Metasequoia glyptostroboides Hu et Cheng, Transcriptome, Endogenous hormones, Adventitious root

Posted Date: July 8th, 2024

DOI: https://doi.org/10.21203/rs.3.rs-4596514/v1

License: This work is licensed under a Creative Commons Attribution 4.0 International License.
Read Full License

Additional Declarations: No competing interests reported.

Version of Record: A version of this preprint was published at BMC Genomics on November 18th, 2024.
See the published version at https://doi.org/10.1186/s12864-024-10989-6.

Abstract

Background

The extract from *Metasequoia glyptostroboides* Hu et Cheng, a rare and endangered species native to China, exhibits numerous biological and pharmacological activities. The species is recalcitrant to rooting during micropropagation, a challenge that has yet to be resolved. In this study, transcriptomic and hormonal analyses were conducted to appreciate the molecular mechanism of adventitious root (AR) formation in optimized rooting conditions.

Results

The use of 2/5-strength Woody Plant Medium (WPM) significantly promoted AR formation of *M. glyptostroboides* shoots while the content of endogenous auxin, cytokinins and gibberellins (GAs) varied at different stages of AR formation. Transcriptomic analysis showed the significant up- or down-regulation of differentially expressed genes (DEGs) associated with plant hormone signal transduction and the phenylpropanoid biosynthesis pathway in response to 2/5-strength WPM. DEGs related to the biosynthesis of indole-3-acetic acid, cytokinins and GAs were identified. Transcript factors involved in 13 families were also revealed. A weighted gene co-expression network analysis indicated a strong correlation between hormones and genes involved in plant hormone signal transduction and the phenylpropanoid biosynthetic pathway.

Conclusions

These results indicate that the AR-promoting potential of 2/5-strength WPM in *M. glyptostroboides* was due to complex interactions between hormones and the expression of genes related to plant hormone signal transduction and the phenylpropanoid biosynthetic pathway.

Background

Roots are an essential element of plant growth as they provide water and nutrients while providing structural support. Adventitious roots (ARs), which form from non-root tissue post-embryonically, are crucial for the establishment of a rooting system for plants [1, 2], and are the main developmental path by which plantlets form roots during vegetative propagation [3]. ARs can form during vegetative propagation with or without stimulation by plant growth regulators (PGRs), typically auxins [4, 5]. ARs also enhance plants' adaptation to adverse environmental conditions and abiotic stresses [6–8]. *In vitro* propagation is an important technology for plant conservation because it allows for the mass propagation and regeneration of elite germplasm. However, it is not uncommon to observe recalcitrance in rooting, especially of woody plants, as has been observed for *Berberis aristata* DC. [9], magnolia [10],

Cariniana legalis [11], and *Pinus koraiensis* Sieb. et Zucc. [12]. Therefore, the ability to induce ARs is a key objective for improving the recalcitrance of *in vitro* rooting in difficult-to-root species.

Several factors can optimize AR induction, including PGRs type and concentration [13], light [14], temperature [15], and other factors. Nutrient deficiency can also serve as a cue for the initiation and elongation of ARs. For example, low phosphorus content increased AR formation in *Solanum lycopersicum* [16], *Populus ussuriensis* [17], and *Malus domestica* [18]. The deficiency of Mn or Fe during the AR induction phase promoted more and longer roots in *Eucalyptus globulus* cuttings [19]. While previous studies on nutrient deficiency-induced AR development centered on a single nutrient, little research has been conducted on the impact of multiple nutrient deficiency. *In vitro* propagation often involves a complex mixture of macro- and micro-nutrients, in the form of a basal medium, whose strength can impact the induction of ARs. Therefore, the adjustment of basal medium strength is a simple but effective way to adjust the molar concentrations of several nutrients simultaneously. For example, the use of different strengths of a popular basal medium, Murashige and Skoog (MS), showed an AR formation gradient from *Echinodorus* 'Indian Red' shoots: 1/2 > 3/4 > 1/4 > full-strength [20], or 1/2 > 3/4 > full > 1/4-strength for *Ledebouria revoluta* bulblets [21]. Half-strength Woody Plant Medium (WPM) [22] free of PGRs induced significantly more ARs from *Salix tetrasperma* shoots than full-strength WPM [23].

The accumulation and distribution of endogenous hormones in plants tend to change in response to exogenous hormones or other factors, resulting in AR formation. In *Malus hupehensis* (Pamp.) Rehd., stem cuttings exogenously treated with indole-3-acetic acid (IAA) significantly accelerated the synthesis of endogenous IAA, gibberellic acid 3 (GA_3), and zeatin riboside (ZR), sped up the metabolism of carbohydrates and soluble proteins, leading to more rapid AR formation [24]. After treating *Vaccinium corymbosum* L. cuttings with indole-3-butyric acid (IBA), endogenous IAA increased significantly at the root primordium formation stage whereas GA_3 content did not change significantly, while the contents of abscisic acid (ABA) and ZR were significantly lower than the control group, suggesting that higher IAA and lower ABA and zeatin contents might facilitate AR formation and development [25]. In stem micro-cuttings of *Malus prunifolia* var. 'Ringo', an apple rootstock, darkness promoted AR formation by increasing or suppressing the endogenous content of IAA, ZR, ABA, GA_3, brassinolide and jasmonic acid (JA) at different stages [26]. In summary, the ability to regulate endogenous hormone content is an essential strategy in the control of AR formation.

Alongside the fluctuation in endogenous hormones, various key genes, proteins and pathways are involved in AR development [27–30]. Transcriptome sequencing revealed that most candidate genes involved in AR formation encoded polar auxin transport carriers, auxin-regulated proteins, and cell wall remodeling enzymes, leading to an enrichment of the biosynthesis of secondary metabolites, plant hormone signal transduction, starch and sucrose metabolism, and other metabolic processes [31–34]. In the absence of PGRs and other growth regulators, genes related to the synthesis, transport, metabolism and recognition of plant hormones were involved in AR formation from *Populus euramericana* micro-cuttings [35]. Red light promoted AR formation in *Camellia gymnogyna* Chang cuttings due to a complex

interaction of hormones and regulation of the expression of genes participating in the response to hormones, cellular glucan metabolism, auxin, and other metabolic processes [36]. Despite these advances in understanding basic and more complex molecular mechanisms underlying AR induction and formation, *in vitro* rooting remains recalcitrant in some woody species.

Metasequoia glyptostroboides Hu et Cheng (Cupressaceae), a known living fossil endemic to southeast China, is a large deciduous conifer. Living individuals of *M. glyptostroboides* were first discovered in the early 1940s in western Sichuan, China, and subsequent population studies revealed that the tree only grows in Sichuan, Hunan, and Hubei provinces [37, 38]. However, given the importance and socio-economic value of its wood, *M. glyptostroboides* was successfully cultivated in Asia, Africa, Europe, and North America [39]. *M. glyptostroboides* has remained genetically unchanged for millions of years and survived extreme ecological and climatic changes since the Cretaceous period [40]. Extracts from *M. glyptostroboides* displayed numerous biological and pharmacological activities, including antioxidant, antidermatophytic [41], antifungal [42], anticancer [43], and anti-amyloidogenic [44]. Due to the limited distribution and declining number of native individual trees found in natural stands, *M. glyptostroboides* was listed as a Class I rare and endangered species in the List of Chinese Rare and Endangered Plants about 30 years ago [45]. It is also classified as an endangered species on the IUCN Red List of Threatened Species [46]. *M. glyptostroboides* seeds are scarce due to the occurrence of male and female cones on different branches of adult trees, and a long juvenile phase before female buds appear [47]. Therefore, the propagation of *M. glyptostroboides* is the main limiting factor for further research development of this living fossil tree.

In a previous study, we developed a shoot-based micropropagation protocol for *M. glyptostroboides*. When treated with either IAA, IBA or 1-naphthaleneacetic acid (NAA), *M. glyptostroboides* shoots showed limited rooting and root number on full-strength WPM after culture for 2 months [48]. Thus, the objectives of this study were to optimize AR induction of *M. glyptostroboides* shoots and attempt to reveal the mechanism underlying AR formation using transcriptomic and hormone analyses.

Results

Adventitious root formation

During *in vitro* rooting, the absence of WPM or the use of low-strength WPM significantly promoted adventitious rooting of *M. glyptostroboides* shoots, when compared with the control group (full-strength WPM) (Fig. 1). The rooting percentage (Fig. 1b), average root number (Fig. 1c) and root length (Fig. 1d) increased significantly in low-strength WPM, and 2/5-strength WPM most effectively induced ARs, resulting in the highest rooting percentage (84.17%), root number (5.67), and root length (3.30 cm) after 30 d of treatment. Histological analysis (Fig. 2) showed that AR initiation was observed after 8 d in 2/5-strength WPM, evidenced by clusters of meristematic cells in the outer phloem. AR primordia were evident at 10 d, and ARs emerged from the epidermis at 12 d and elongated after 16 d. In the control, no AR primordia were observed between 8 and 10 d, only after 12 d. AR primordia emerged from the

epidermis at 16 d and elongated at 20 d. Thus, the base of shoots (0.5-1.0 cm) collected at 8, 10, 12, 16, and 20 d from 2/5-strength WPM (marked as MG) and control (CK) were employed as the samples for endogenous hormone content and RNA-seq analysis.

Analysis of endogenous hormone content

Nine endogenous hormones, IAA, isopentenyladenine (IP), isopentenyladenosine (IPA), *trans*-zeatin riboside (TZR), *trans*-zeatin (TZT), GA_1, GA_3, GA_4 and GA_7, at 8, 10, 12, 16, and 20 d in MG and CK were detected in the stem bases of *M. glyptostroboides* (Fig. 3). Endogenous IAA mainly accumulated at 12 d, and levels at 8, 10, 12, 16, and 20 d in the control were significantly higher than in all MG treatments. There was no significant difference in IP content between MG and CK, except at 10 d. IPA content in MG was significantly lower than in CK, except at 16 d. TZR in stems accumulated from 8 to 20 d in MG and CK, and in MG was significantly higher than in CK at 20 d. TZT, GA_1 and GA_3 accumulated rapidly at 16 and 20 d in MG and CK (GA_1 was not detected at 8–12 d). TZT content in MG was significantly higher than in CK at 20 d, whereas GA_1 and GA_3 contents were significantly lower in MG at 16 and 20 d. GA_4 content increased sharply at 12 d, corresponding to the timing of ARs breaking through the epidermis in MG, then decreased rapidly at 16 and 20 d, corresponding to the timing of AR elongation. Unlike MG, CK displayed a significantly higher level of GA_4 at 16 and 20 d, corresponding to the timing of AR primordia formation and breaking through the epidermis. Compared with CK, GA_7 content in MG showed no significant difference at 8 and 10 d, but was significantly lower at 12, 16 and 20 d, corresponding to the stage of ARs breaking through the epidermis and extension.

In brief, 2/5-strength WPM induced AR formation from *M. glyptostroboides* stems, displaying a lower endogenous content of IAA, TZT, GA_1, GA_3 and GA_7 at different stages, except TZT at the late stage of AR extension (20 d). At the stage of AR primordia formation (10 d) and breaking through the epidermis (12 d), stems showed lower contents of IP, IPA and TZR, and higher GA_4 content at 12 d. At the early stage of AR elongation (16 d), stems showed a lower content of GA_4 and higher contents of IPA and TZR. At the late stage of AR extension (20 d), a higher content of TZT was observed in stems.

Analysis of RNA sequences and identification of differentially expressed genes (DEGs)

To identify genes involved in AR formation from *M. glyptostroboides* stem bases, 30 cDNA libraries were prepared from three repeat mRNA samples collected from the 2/5-strength WPM treatment (MG) and the control (CK) at 8, 10, 12, 16 and 12 d, marked as MG8, MG10, MG12, MG16, MG20 and CK8, CK10, CK12, CK16, CK20, respectively. The sequenced raw data was submitted to the SRA at the NCBI database with the following accession number: PRJNA999065. The total number of raw reads obtained for each library ranged from 49,120,012 to 70,131,470 with Q20 > 97.32% and Q30 > 93.17% (Table 1). After filtering, the number of clean reads per library ranged from 48,871,938 to 69,828,774 (Table 1).

When the stems of *M. glyptostroboides* placed in 2/5-strength WPM and control medium were compared, 253 (MG8 vs CK8), 239 (MG10 vs CK10), 417 (MG12 vs CK12), 540 (MG16 vs CK16), and 364

(MG20 vs CK20) DEGs were identified on days 8, 10, 12, 16 and 20, respectively (Fig. 4a). The highest number of up-regulated genes was observed in the MG16 vs CK16 library (330) and fewest in the MG10 vs CK10 library (99) (Fig. 4a). The Venn diagram indicates that three genes maintained significant differential expression in the 2/5-strength WPM treatment from between 8 and 20 d (Fig. 4b).

GO and KEGG enrichment analysis of DEGs

The significant enrichment GO terms of DEGs showed a few differences in the five compared libraries (Fig. S1). In MG8 vs CK8, the significantly enriched terms were “glutamate catabolic process”, “dicarboxylic acid catabolic process”, “xyloglucan: xyloglucosyl transferase activity”, “xyloglucan metabolic process”, etc. In MG10 vs CK10, the most significantly enriched terms were “sexual reproduction”, “reproduction”, “mannose binding”, etc. In MG12 vs CK12, “dipeptide transmembrane transporter activity”, “tripeptide transmembrane transporter activity” and “cell wall”, etc. were indicated as being the most significantly enriched terms. In MG16 vs CK16, “lactoperoxidase activity”, “hydrogen peroxide catabolic process”, “hydrogen peroxide metabolic process”, etc. were the main significantly enriched terms. In MG20 vs CK20, the most significantly enriched terms were “sexual reproduction”, “reproduction”, “xyloglucan metabolic process”, etc. The KEGG pathways significantly enriched in each stage displayed a significant difference between each treatment (Fig. S2). In MG8 vs CK8, the significantly enriched DEG pathways were “taurine and hypotaurine metabolism”, “butanoate metabolism”, “alanine, aspartate and glutamate metabolism”, “plant hormone signal transduction”, etc. In MG10 vs CK10, DEGs in “arginine and proline metabolism” and “vitamin B6 metabolism” pathways were significantly enriched. In MG12 vs CK12 and MG16 vs CK16, “phenylpropanoid biosynthesis” was the most significantly enriched pathway. In MG20 vs CK20, “plant hormone signal transduction” and “pentose and glucuronate interconversions” pathways were the most significantly enriched.

DEGs enriched in the plant hormone signal transduction pathway

KEGG pathway enrichment analysis showed that 34 DEGs were enriched in the “plant hormone signal transduction” pathway, including genes encoding IAA-amido synthetase Gretchen Hagen3 (*GH3*), auxin/IAA (*AUX/IAA*), Protein TIFY 10b (*TI10B*), pathogenesis-related protein (*PR*), auxin-responsive proteins (*SMALL AUXIN UP RNA*, *SAUR*), and xyloglucan endotransglucosylase protein (*XTH*) (Fig. 5). Three *GH3* genes were identified, one of which (Mgl0097120) was exclusively up-regulated in MG16 vs CK16 and two (Mgl0098450 and Mgl0097090) that were differentially expressed in MG20 vs CK20. Only one *IAA27* gene (Mgl0010460) was identified; it was significantly up-regulated in MG12 vs CK12 and MG16 vs CK16. Four DEGs encoding jasmonate ZIM domain-containing protein (*JAZ*) were significantly up-regulated in MG8 vs CK8 and MG16 vs CK16, respectively, including three *TI10B* DEGs (Mgl0152960, Mgl0211930, Mgl0211910) and one hypothetical protein (Mgl0211950). Four *SAUR* and three *PR1* DEGs showed differential expression in MG8 vs CK8 (Mgl0056630, *SAUR12*), MG12 vs CK12 (Mgl0056630, *SAUR12*; Mgl0266300, Mgl0240770, *PR1*), MG16 vs CK16 (Mgl0056790, *SAUR*; Mgl0222810, *SAUR71*; Mgl0266300; Mgl0240770; Mgl0240810, *PR1*) and MG20 vs CK20 (Mgl0038910, *SAUR32*; Mgl0240770, *PR1*). Nineteen *XTH* DEGs were identified, but only four *XTH1* (Mgl0287740, Mgl0287830, Mgl0287700,

Mgl0287730) and one *XTH34* (Mgl0097340) were significantly up-regulated in MG8 vs CK8, two *XTH1* (Mgl0287710 and Mgl0287780) in MG20 vs CK20, one *XTH1* (Mgl0282260) and one *XTH5* (Mgl0289590) in MG16 vs CK16, nine *XTH1* (Mgl0287680, Mgl0287690, Mgl0287720, Mgl0287750, Mgl0287760, Mgl0287870, Mgl0287860, Mgl0287850, and Mgl0287880) in MG8 vs CK8 and MG20 vs CK20, and one *XTH1* (Mgl0287840) in MG8 vs CK8, MG16 vs CK16 and MG20 vs CK20 (Table S1).

DEGs enriched in the phenylpropanoid biosynthesis pathway

A total of 52 peroxidase (*PER*) DEGs were enriched in the "phenylpropanoid biosynthesis" pathway, most of which were differentially expressed in MG12 vs CK12 and MG16 vs CK16, corresponding to the stage of AR emergence from the epidermis and elongation (Fig. 6, Table S2). Ten out of 52 *PER* DEGs were significantly down-regulated in MG8 vs CK8 (Mgl0266600, *PER12*), MG10 vs CK10 (Mgl0017650, *PER4*), MG12 vs CK12 (Mgl0266600; Mgl0004180, *PER2*; Mgl0037470, *PER25*; Mgl0017750, *PER1*; Mgl0017650, *PER4*), MG16 vs CK16 (Mgl0266600; Mgl0004180; Mgl0017210, *PER12*; Mgl0272220, *PER5*; Mgl0017750; Mgl0017760, *PER70*), and MG20 vs CK20 (Mgl0004180; Mgl0173900, *PER51*; Mgl0202410, *PER66*). *PER19* (Mgl0077730) was initially significantly up-regulated in MG12 vs CK12, then decreased significantly in MG20 vs CK20, while two *PER5* (Mgl0272180 and Mgl0272230) were down-regulated in MG16 vs CK16 then up-regulated in MG20 vs CK20. Thirty-nine out of 52 *PER* DEGs were up-regulated at different stages, 10 of which were exclusively significantly up-regulated (Mgl0272300, *PER5*; Mgl0017540, *PER4*; Mgl0016520, *PER27*; Mgl0184200, *PER1*; Mgl0125520, *PER3*; Mgl0167670, *PER56*; Mgl0294200, *PER5*; Mgl0016070, *PER3*; Mgl0167660, *PER27*; Mgl0219990, *PER3*) in MG12 vs CK12, nine (Mgl0017510, *PER4*; Mgl0141010, *PER39*; Mgl0008240, *PER47*; Mgl0114430, *PER2*; Mgl0016530, *PER56*; Mgl0141000, *PER3*; Mgl0056040, *PER51*; Mgl0121310, *PER55*; Mgl0125510, *PER3*) in MG16 vs CK16, and five (Mgl0263220, *PER5*; Mgl0017630, *PER52*; Mgl0017200, *PER12*; Mgl0272210, *PER5*; Mgl0017790, *PER4*) in MG20 vs CK20. Three *PER* DEGs (Mgl0017780, *PER1*; Mgl0016080, *PER3*; Mgl0272310, *PER5*) were significantly up-regulated at 8 d, and Mgl0272310 (*PER5*) and Mgl0016080 (*PER3*) were significantly up-regulated at 10 and 12 d, respectively. Seven *PER* DEGs (Mgl0068470, *PER5*; Mgl0017520, *PER4*; Mgl0305250, *PER1*; Mgl0134470, *PER27*; Mgl0037420, *PER28*; Mgl0178090, *PER4*; Mgl0016510, *PER39*) were significantly up-regulated at 12 and 16 d in MG, relative to CK. Mgl0016480 (*PER39*) and Mgl0178150 (*PER4*) were significantly up-regulated in MG8 vs CK8, MG12 vs CK12 and MG16 vs CK16. Similarly, Mgl0017890 (*PER1*) was significantly up-regulated in MG16 vs CK16 and MG20 vs CK20. Mg10016500 (*PER56*) was significantly up-regulated at 10, 12 and 16 d in MG, compared with CK. Mgl0282530 (*PER72*) was significantly up-regulated from 8 to 16 d in MG vs CK.

In addition, one DEG for an aldehyde dehydrogenase family 2 member B4 gene (*ALDH2B4*), one caffeic acid 3-*O*-methyltransferase gene (*COMT1*), one *trans*-cinnamate 4-monooxygenase C4H2 gene (*C4H2*), one acyltransferase GLAUCE (*GLC*) gene, and two cinnamoyl-CoA reductase 1 (*CCR*) genes (Fig. 6, Table S2) were enriched in the "phenylpropanoid biosynthesis" pathway. *ALDH2B4* (Mgl0101560) was significantly up-regulated in MG16 vs CK16. *C4H2* (Mgl0012640) was significantly up-regulated in MG8 vs CK8 and MG20 vs CK20, and down-regulated in MG12 vs CK12. *GLC* (Mgl0271670) was significantly

down-regulated in MG16 vs CK16. *CCR* (Mgl0131050 and Mgl0131240) was significantly up-regulated in MG8 vs CK8, and *COMT1* (Mgl0247750) in MG12 vs CK12.

DEGs enriched in tryptophan metabolism, diterpenoid biosynthesis and zeatin biosynthesis pathways

Four DEGs were enriched in the “tryptophan metabolism” pathway, which is involved in IAA biosynthesis, including genes encoding proteins for indole-3-pyruvate monooxygenase (*YUC2*) (Mgl0088070), acetylserotonin *O*-methyltransferase (*ASMT*) (Mgl0116960 and Mgl0209550), and *COMT1* (Mgl0247750) (Fig. 7a, Table S3). Mgl0088070 was significantly down-regulated in MG12 vs CK12. Mgl0116960 (*ASMT*) was significantly up-regulated in MG16 vs CK16 whereas Mgl0209550 (*ASMT*) was significantly down-regulated in MG10 vs CK10. One DEG (Mgl0229440, *ent*-kaur-16-ene synthase, *KS1*) involved in gibberellin biosynthesis was enriched in the “diterpenoid biosynthesis” pathway, and was significantly up-regulated in MG16 vs CK16 (Fig. 7b, Table S3).

One DEG related to zeatin *O*-xylosyltransferase (*ZOX1*) (Mgl0264320), two *cis*-zeatin *O*-glucosyltransferase 1 (*CISZOG1*) DEGs (Mgl0049820 and Mgl0049830) and three scopoletin glucosyltransferase (*TOGT1*) DEGs (Mgl0307290, Mgl0063030 and Mgl0062950) were enriched in the “zeatin biosynthesis” pathway; these regulated the biosynthesis of TZT, TZR, IP and IPA (Fig. 7c and Table S3). *ZOX1* (Mgl0264320) was significantly down-regulated in MG8 vs CK8 and MG16 vs CK16. Two *CISZOG1* were significantly up-regulated in MG12 vs CK12, and Mgl0049830 (*CISZOG1*) was also significantly up-regulated in MG10 vs CK10. Three *TOGT1* DEGs showed considerable differential expression patterns in different comparison groups: Mgl0307290 (*TOGT1*) was up-regulated in MG16 vs CK16; Mgl0063030 (*TOGT1*) was up-regulated in MG12 vs CK12 and down-regulated in MG20 vs CK20; Mgl0062950 (*TOGT1*) was up-regulated in MG16 vs CK16 and MG20 vs CK20.

Transcript factors (TFs) analysis

A total of 31 DEGs were identified as TF, and were classified into 13 families with reference to the PlantTFDB, including 9 MYB (v-MYB avian myeloblastosis viral oncogene homolog), 4 NAC (NAM/ATAF/CUC protein), 3 AP2 (APETALA2), 3 bHLH (basic helix-loop-helix domain protein), 2 ERF (Ethylene responses factor), 2 MYB-related, 2 WRKY, 1 GRAS (Glycopeptide resistance-associated protein), 1 HB-other (Homeobox-other), 1 HSF (Heat stress transcription factor), 1 LBD (Lateral organ boundaries domain protein), 1 YABBY and 1 bZIP (basic leucine zipper domain protein) (Fig. S3 and Table S4) TF. Most of those DEGs were not annotated in a certain pathway, except the bZIP. Among those DEGs, eight out of nine MYB were significantly up-regulated in MG8 vs CK8, MG12 vs CK12, MG16 vs CK16 and MG20 vs CK20 group, respectively, indicating a potential positive role in meristematic cells and AR formation, and AR elongation of *M. glyptostroboides*.

Co-expression network analysis by weighted gene co-expression network analysis (WGCNA)

To explore the relationship between phytohormone content and gene expression in *M. glyptostroboides* AR formation, a co-expression network was constructed by WGCNA. The modules in WGCNA are defined as clusters of highly interconnected genes, and genes in the same cluster have a high correlation coefficient. Five modules had a highly positive correlation with phytohormone content. Among them, the correlation coefficient between MEblue with TZT and GA_1 was high (0.737 and 0.771, respectively) (Fig. 8a). MEturquoise had a highly positive correlation (R = 0.565, $p = 0.00$) with IAA, but had highly negative correlations with TZT (R = -0.856, $p = 0.0$) and GA_1 (R = -0.841, $p = 0.00$) (Fig. 8a). MEred had a highly positive correlation with GA_4 (Fig. 8a). MEbrown had positive correlations with IP, TZT, TZR, GA_1 and GA_3 (Fig. 8a). MEblack had positive correlations with IP, IPA, TZT, TZR, GA_1, GA_3 and GA_7 (Fig. 8a). According to the related phytohormone components in other modules and correlations, MEblack, MEblue and MEturquoise were selected for network model analysis.

The genes with top 500 connectivity were selected to perform further analysis. The hub genes are those that show high connectivity in a network. In the MEblack module, 118 genes were identified with high expression in the control group (Fig. 8b). Genes encoding Receptor-like protein EIX2, L-gulonolactone oxidase 5, α-amylase, glutathione *S*-transferase U7, endochitinase 4 and xanthotoxin 5-hydroxylase CYP82C4 were identified as candidate hub genes for this module. Those genes were involved in “plant-pathogen interaction”, “ascorbate and aldarate metabolism”, “biosynthesis of cofactors”, “starch and sucrose metabolism”, glutathione metabolism”, “amino sugar and nucleotide sugar metabolism” and “isoflavonoid biosynthesis” pathways, respectively (Table 2). A total of 1080 genes with high expression at the AR elongation stage (CK20, MG16, MG20) (Fig. 8c) were categorized into the MEblue module, and several genes involved in “phenylpropanoid biosynthesis”, “plant hormone signal transduction”, “MAPK signaling pathway - plant”, “plant-pathogen interaction”, “tryptophan metabolism” and “zeatin biosynthesis” pathways, including *PER*, *PR1*, *XTH*, *ASMT* and *CISZOG1*, were identified as candidate hub genes for this module (Table 2). A total of 1467 genes with high expression at the AR initiation phase (MG8) or the stages in which no AR primordia with potential meristematic cells were observed (CK8, CK10) (Fig. 8d) were identified in the MEturquoise module. Three candidate hub genes (*PER*, *GLC*, *KS1*) were involved in “phenylpropanoid biosynthesis” and “diterpenoid biosynthesis” pathways (Table 2).

Reverse transcription quantitative polymerase chain reaction (RT-qPCR) analysis of gene expression

To further validate the RNA-seq results, eight candidate DEGs (four DEGs (Mgl0010460, *IAA27*; two *XTH1*, Mgl0287720 and Mgl0287740; Mgl0289590, *XTH5*) enriched in the “plant hormone signal transduction” pathway; two DEGs (Mgl0141010, *PER39*; Mgl0167670, *PER56*) enriched in the “phenylpropanoid biosynthesis” pathway; *TOGT1* (Mgl0063030) and *CISZOG1* (Mgl0049820) enriched in the “zeatin biosynthesis” pathway) were selected for RT-qPCR analysis of *M. glyptostroboides* stems that were collected from 2/5-strength WPM and control medium at 8, 10, 12, 16 and 20 d. The expression trends of the DEGs from qRT-PCR and RNA-seq analysis were largely consistent (Fig. 9). In addition, correlation analysis showed that the RNA-seq results were highly consistent ($R^2 = 0.8083$) with the RT-

qPCR results (Fig. 9), demonstrating that the transcriptome data was reliable to reflect the response of 2/5-strength WPM-induced AR formation of *M. glyptostroboides* plantlets.

Discussion

Rooting recalcitrance has been a major limitation in the vegetative propagation of elite plant germplasm [49–51]. In general, PGRs can effectively induce or promote AR formation, combined with or without other regulators, and are the dominant factor affecting AR induction in the clonal propagation of many plant species [52–54]. However, the inducible ability of PGRs is insufficient in some difficult-to-root species. The effect of nutrient deficiency on AR formation has been reported in many plant species, especially crops [55, 56]. Nutrient deficiency-induced stress stimulated AR growth, by increasing the available root surface area and contributing to nutrient uptake [3]. In the present study, low-strength WPM significantly promoted AR formation from *M. glyptostroboides* stems. Compared with full-strength WPM, after elongation on WPM medium, plantlets likely experienced nutrient deficiency-induced stress during low strength WPM-induced AR formation. Thus, 2/5-strength WPM-promoted AR formation in *M. glyptostroboides* plantlets might serve as a response to nutrient deficiency. The low cost and efficient rooting promoted by the use of low ionic strength of the basal culture medium is a candidate strategy for the induction and formation of ARs in the micropropagation systems of difficult-to root species.

Phytohormones, as physiological signals that regulate plant growth and development, are very important for AR development. There have been many reports dedicated to the accumulation patterns of endogenous IAA, cytokinins and GAs during AR formation. It is widely accepted that IAA is the central player that induces AR in competent cells, and an increase in IAA content is always observed over the course of rooting [57–59], as a result of the expression of multiple genes involved in the maintenance of auxin homeostasis [60–62]. Cytokinins, including IP, IPA, TZR and TZT, are thought to have an early positive regulative function at the stage of dedifferentiation during AR formation, whereas high concentrations of cytokinins act antagonistically to auxin during the induction phase [58, 63, 64]. GAs may have an AR phase-dependent effect, being inhibitory to root induction and stimulatory to AR formation in some species [52, 63]. For *M. glyptostroboides* plantlets, 2/5-strength WPM-promoted rooting displayed a lower level of endogenous IAA and cytokinins than the control. Similar findings were observed during adventitious rooting of *Camellia sinensis* cuttings [65] and *Picea abies* seedlings [66]. In addition, a lower level of GA_1, GA_3 and GA_7 over the entire rooting process of *M. glyptostroboides* plantlets was revealed in 2/5-strength WPM-promoted rooting, confirming the hypothesis that high levels of GA negatively regulate AR formation [67], and suggesting species- or treatment-dependent phytohormone accumulation patterns during AR formation. In this study, during AR formation in *M. glyptostroboides* plantlets, genes in tryptophan metabolism, diterpenoid biosynthesis and zeatin biosynthesis pathways showed differential expression patterns, alongside a fluctuation in IAA, IP, IPA, TZR, TZT and GA content. These results suggest a module in which low-strength WPM induced ARs in *M. glyptostroboides* plantlets by regulating the level of phytohormones and the expression of phytohormone-related genes.

Generally, AR formation is inseparable from the regulation of plant hormone signal transduction [68–70]. Multiple plant hormone signal transduction-related genes are involved in adventitious rooting. GH3, AUX/IAA and SAUR are early auxin response proteins that are active during AR formation. GH3 plays a crucial role in conjugating IAA to amino acids, and is critical in maintaining auxin homeostasis [71–73]. AUX/IAA always participates in the auxin signaling pathway by interacting with auxin response factor protein or other genes [74–76]. SAURs mediate the regulation of several aspects of plant growth and development, and have positive or negative effects on primary, lateral and adventitious root development [77–80]. In *M. glyptostroboides*, *GH3*, *IAA*, and *SAUR* DEGs were significantly enriched in plant hormone signal transduction, implying a link to AR induction of *M. glyptostroboides* plantlets. Furthermore, numerous *XTH* DEGs that were significantly enriched in plant hormone signal transduction were also differentially expressed. XTH, belonging to glycoside hydrolase family 16, is a key enzyme in plant cell wall remodeling and a cell-wall-loosening protein involved in cell expansion or cell-wall weakening [81]. In marigold explants, methane-rich water and 2,4-epibrassinolide significantly promoted the activity of two major cell wall-relaxing factors, XTH and peroxidase, which in turn promoted AR formation [82]. However, an understanding of the direct relationship between *XTH* expression and AR formation is still limited. *XTH* might be an excellent candidate for future biotechnological efforts to improve rooting in some plant species.

Phenylpropanoid biosynthesis has been identified as a remarkable pathway of AR formation in several species [70, 83, 84]. In this study, phenylpropanoid biosynthesis was also analyzed as a significantly enriched pathway during the stage of AR emergence from the epidermis and elongation, with a number of *PER* DEGs having been identified. *PER* encodes peroxidase (E1.11.1.7), which plays an important role in a number of physiological processes in plants, are heme-containing enzymes with catalytic action on diverse organic compounds, including IAA, and their activity has been used as a biochemical marker of rooting [85]. In basal tissue of *Saccharum spp*. interspecific hybrids microshoot, the altered expression of *PER* genes involved in phenylpropanoid biosynthesis during AR formation might cause alterations in the production of lignin and many functional compounds involved in various processes associated with cell division and organogenesis [70]. Therefore, *PER* could be considered as a crucial DEG in AR formation.

WGCNA is a useful approach for identifying sample-specific modules and candidate hub genes in plant growth and development [86–88]. The hub genes in adventitious rooting have been revealed by WGCNA analysis for some plant species. In *Camellia sinensis* (L.) O. Kuntze cuttings, hub genes involved in NAA-mediated AR formation were identified by WGCNA, such as Helix-loop-helix DNA-binding Domain transcription factor, AP2 domain (AP2)-containing protein, *SAUR*, etc. [65]. In *C. gymnogyna* Chang, WGCNA analysis identified three highly correlated modules and hub genes mainly participated in “response to hormone”, “cellular glucan metabolic progress” and “response to auxin” during AR development under red light [36]. A total of nine co-expression modules were constructed in this study, including three modules that were significantly related to phytohormone content in AR development of *M. glyptostroboides* plantlets. The candidate hub genes were involved in plant hormone signal transduction and phenylpropanoid biosynthesis pathway. These findings suggest a complex interaction

between hormones and the expression of genes related to the above two pathways in AR formation of *M. glyptostroboides* plantlets.

Conclusion

In this research, the use of 2/5-strength WPM promoted AR development from *M. glyptostroboides* stems. The contents of endogenous auxins, cytokinins and GAs changed dramatically at different stages of AR formation. The AR-promoting potential of 2/5-strength WPM for *M. glyptostroboides* is due to complex interactions between hormones and the expression of genes related to plant hormone signal transduction and phenylpropanoid biosynthesis pathway. The knowledge gained from this study will help researchers better understand the molecular traits of low strength basic culture medium-based regulation of adventitious rooting of *M. glyptostroboides* plantlets. A hypothetical model of adventitious root formation of *M. glyptostroboides* plantlets based on our results is shown in Fig. 10.

Methods

Adventitious root induction

This study employed the micropropagation system and culture conditions for *M. glyptostroboides* that were previously established [48]. *In vitro* plantlets were maintained and propagated on WPM supplemented with 5.0 μM 6-benzyladenine (BA) (Solarbio, Beijing, China). Single shoots (1 cm in height) cut from multiple *in vitro* shoots were inoculated on PGR-free WPM for 30 d. ARs were not induced during this period. For the rooting treatment, after trimming 2 mm from the base of single shoots (each containing four leaves and two nodes) cultured on PGR-free WPM for 30 d, trimmed shoots were inoculated onto 0, 1/5, 2/5, 4/5 or full-strength WPM supplemented with 0.05 μM NAA (Macklin, Shanghai, China), 10 g/L sucrose and 0.5% (w/v) agar. The 0-strength WPM treatment contained only 10 g/L sucrose and 0.5% (w/v) agar. The full-strength WPM treatment was used as the control (CK). Ten shoots were placed in each jar (four jars per treatment). Three replicates were performed for each treatment (n = 12 jars; total = 120 shoots). Rooting percentage, average root number and root length were calculated for each treatment after 30 d. Significant differences in each parameter between treatments were analyzed by Duncan's multiple range test ($p \leq 0.05$) after mean separation using one-way analysis of variance.

Histological analysis

At least 15 bases of *M. glyptostroboides* shoots (0.5-1.0 cm) from the control and optimized rooting treatments were collected at 8, 10, 12, 16, and 20 d and fixed in formalin/acetic acid/alcohol (50% ethanol: 37% formalin: glacial acetic acid, 18:1:1, v/v/v) at 25 ± 2°C for > 24 h. After dehydrating shoot bases in a 70–100% alcohol series, fixed material was infiltrated with, and embedded in molten paraffin wax (Sinopharm, Beijing, China). Sections (4–6 μm thick) for microscopy were made with a Leica

RM2255 (Wetzlar, Germany) rotary microtome and stained in 0.5% fast green (Sinopharm). Micrographs were obtained with a Nikon Eclipse E200 microscope (Nikon, Tokyo, Japan) and HQimage C630 digital camera (Hengqiao, Hangzhou, China).

Determination of endogenous hormones

To analyze the content of endogenous hormones, the same material employed for histological analysis was used, and stored at -80℃. Three biological replicates (20 cut stem bases in each) were harvested (0.2 g fresh weight (FW) for each base) to assess endogenous IAA, GA_1, GA_3, GA_4, GA_7, TZR, TZT, IP, and IPA content by liquid chromatography-tandem mass spectrometry (LC-MS/MS). This analysis was conducted by Wuhan ProNets Biotechnology Co, Ltd. (Wuhan, China). All standards for this analysis were purchased from Sigma (St. Louis, MI, USA), except GA_1 and GA_7, which were purchased from Toronto Research Chemicals (Toronto, Canada). The internal standard mixture was consisted of D-IAA and D-SA, with the concentration of 1μg/mL. The samples were ground to a powder using liquid nitrogen, then 10 volumes of acetonitrile solution and 2 μL of internal standard solution were added to the powder. The mixture was incubated at 4°C overnight, then centrifuged at 12,000 *g* for 5 min with high-speed refrigerated centrifuge (Ke Cheng H3-18KR, Hunan, China). Five volumes of acetonitrile solution were added to the precipitate, which was extracted twice, then supernatants were pooled. After purified with CNW C18 chromatographic packing (CNW, Duesseldorf, Germany), the supernatant was collected and concentrated until dry with a CV600 centrifugal concentrator (Jiaimu, Beijing, China). For analysis, the dried supernatant was suspended in 150 μL methanol and filtered through a 0.22 μm organic phase filter membrane (Jingteng, Tianjin, China). Hormones were measured by high-performance liquid chromatography (HPLC) (Agilent 1290; Santa Clara, CA, USA) with WATERS ACQUITY UPLC HSS T3 (2.1 × 100 mm, 1.8 μm) (Waters, MA, USA) chromatographic column and AB Qtrap6500 mass spectrometer (AB Sciex, Foster City, CA, USA). The analytical mobile phase of HPLC consisted of 0.1% formic acid (mobile A) and acetonitrile (mobile B). The gradient began at 95% A and 5% B for 1.0 min, moving to 5% A and 95% B at 8.0 min, then returning to 95% A and 5% B at 8.1 min, and remaining there to 10.0 min. The flow rate was 0.3 mL/min and the column temperature was set at 30°C. The MS parameters are indicated in Table S5. Following mean separation using one-way ANOVA, significant differences in the content of endogenous hormones between treatments were assessed with the Mann Whitney non-parametric test ($p \leq 0.05$).

Library preparation, sequencing and read mapping

The samples used to analyze the content of endogenous hormones were also employed for RNA-seq analysis. Total RNA was extracted from each sample using TRIzol® reagent according the manufacturer's instructions (Invitrogen, Carlsbad, CA, USA). The quality of total RNA was determined by a 5300 Bioanalyser (Agilent) and quantified using NanoDrop 2000 (Thermo Fisher Scientific, Wilmington, NC, USA). RNA purification, reverse transcription, library construction and sequencing were performed by Shanghai Majorbio Bio-pharm Biotechnology Co., Ltd. (Shanghai, China) according to the manufacturer's instructions (Illumina, San Diego, CA, USA). The paired-end RNA-seq sequencing library was sequenced

with the Illumina NovaSeq 6000. Raw paired end reads were trimmed and quality control was achieved by fastp [89] using default parameters. Clean reads were separately aligned to the reference *M. glyptostroboides* genome [90] in orientation mode using HISAT2 software [91]. The mapped reads of each sample were assembled by String Tie [92] using a reference-based approach.

Differential expression analysis and functional enrichment

The expression levels of genes were calculated as reads per kilobase of transcript sequence per million base pairs sequenced (FPKM). Gene abundance was quantified by RSEM (http://deweylab.biostat.wisc.edu/rsem/) [93]. DESeq2 [94] was used to perform differential expression analysis. DEGs with $|\log_2 FC| \geq 1$ and a false discovery rate (FDR) ≤ 0.05 were considered as significantly differently expressed genes. In addition, functional-enrichment analysis, including the use of Gene Ontology (GO) and Kyoto Encyclopedia of Genes and Genomes (KEGG), was performed to identify which DEGs were significantly enriched, as assessed by GO terms and KEGG pathways, compared with the whole-transcriptome background (Bonferroni-correction; $p \leq 0.05$). GO terms and KEGG pathway enrichment analysis were carried out by Goatools (https://github.com/tanghaibao/Goatools) and KOBAS (http://kobas.cbi.pku.edu.cn/home.do) [95]. Identification of TF families was performed by using BLASTX similarity from the Plant Transcription Factor Database (PlantTFDB v5.0; http://planttfdb.gao-lab.org/) with the default parameters. Gene co-expression networks were constructed with the WGCNA, v 1.63 package [96]. The WGCNA parameters settings were: average FPKM > 1; variable coefficient > 0.1; soft threshold = 10; minimum module size = 30; merge cut height = 0.1; connection value (|KME|) > 0.5.

RT-qPCR analysis

For RT-qPCR analysis, eight candidate DEGs in the enriched KEGG pathway were selected to validate the RNA-seq results. Gene-specific primers are listed in Table S6. The qTower^3 (Analytik Jena, Jena, Germany) and PerfectStart Green qPCR Supermix (TransGen Biotech, Beijing, China) were employed for RT-qPCR. Three biological replicates and three technical replicates were performed for each candidate gene. *M. glyptostroboides* actin was used as the internal control and the differential expression of candidate DEGs was analyzed by the $2^{-\Delta\Delta Ct}$ method [97].

Abbreviations

ABA	Abscisic acid
ALDH2B4	Aldehyde dehydrogenase family 2 member B4 gene
AR	Adventitious root
ASMT	Acetylserotonin *O*-methyltransferase
BA	6-benzyladenine
bHLH	basic helix-loop-helix domain protein
bZIP	basic leucine zipper domain protein
C4H2	*trans*-cinnamate 4-monooxygenase C4H2 gene
CCR	Cinnamoyl-CoA reductase 1
cDNA	Complementary deoxyribonucleic acid
CISZOG	*cis*-zeatin *O*-glucosyltransferase
COMT	Caffeic acid 3-*O*-methyltransferase gene
DEG, DEGs	Differentially expressed gene(s)
FC	Fold change
FPKM	Fragments per kilobases per million mapped reads
FW	Fresh weight
GA, GAs	Gibberellic acid; gibberellins
GH3	IAA-amido synthetase Gretchen Hagen3
GRAS	Glycopeptide resistance-associated protein
GLC	Acyltransferase GLAUCE
GO	Gene ontology
HB-other	Homeobox-other
HSF	Heat stress transcription factor
IAA	Indole-3-acetic acid
IBA	Indole-3-butyric acid
IP	Isopentenyladenine
IPA	Isopentenyladenosine
JA	Jasmonic acid
JAZ	Jasmonate ZIM domain-containing protein

KEGG	Kyoto Encyclopedia of Genes and Genomes
LC-MS/MS	Liquid chromatography-tandem mass spectrometry
LBD	Lateral organ boundaries domain protein
MS	Murashige and Skoog
MYB	v-MYB avian myeloblastosis viral oncogene homolog
NAA	α-naphthaleneacetic acid
NAC	NAM/ATAF/CUC protein
NCBI	National Center for Biotechnology Information
PCR	Polymerase chain reaction
PER	Peroxidase
PGR	Plant growth regulator
PR	Pathogenesis-related protein
RT-qPCR	Reverse transcription quantitative PCR
RNA	Ribonucleic acid
RNA-seq	RNA-sequencing
RSEM	RNA-seq by Expectation Maximization
TOGT	Scopoletin glucosyltransferase
TF	Transcript factor
TZR	*trans*-zeatin riboside
TZT	*trans*-zeatin
WGCNA	Weighted gene co-expression network analysis
WPM	Woody Plant Medium
XTH	Xyloglucan endotransglucosylase protein
YUC	Indole-3-pyruvate monooxygenase
ZOX	Zeatin *O*-xylosyltransferase
ZR	Zeatin riboside

Declarations

Ethics approval and consent to participate

Not applicable.

Consent for publication

Not applicable.

Availability of data and materials

All data during this study are included in this article and its supplementary information files. The RNA-seq data has been deposited in the Sequence Read Archives Database (https://www.ncbi.nlm.nih.gov/sra/) under accession number PRJNA999065 (https://www.ncbi.nlm.nih.gov/sra/PRJNA999065).

Competing interests

The authors declare no competing interests.

Funding

This work was supported by Guangdong Basic and Applied Basic Research Foundation (2021A1515011278)， Science and Technology Projects in Guangzhou (2024A04J4590), Guangdong Science and Technology Plan Project 【2023B1212060046】and National Natural Science Foundation of China Youth Fund (32100311).

Authors' contributions

YPX, GHM, XHZ and SJZ designed the experiment and provided guidance on the study. YPX, XHC and JYL prepared samples for AR induction, hormones contents and RNA-seq analysis. JRL, YL and ZB participated in the experiment of AR induction and anatomical analysis. YPX and GHM were involved in statistical analyses and co-wrote the manuscript. JATS provided advice for the experiment, interpretation of the results, assisted with analyses, and co-wrote the manuscript with GHM. All authors read and approved the manuscript for publication.

Acknowledgements

Not applicable.

References

1. Barlow PW: Adventitious roots of whole plants: their forms, functions, and evolution. In: New Root Formation in Plants and Cuttings. Edited by Jackson MB. Dordrecht: Springer Netherlands; 1986: 67-110.
2. Rasmussen A, Hosseini SA, Hajirezaei MR, Druege U, Geelen D. Adventitious rooting declines with the vegetative to reproductive switch and involves a changed auxin homeostasis. J Exp Bot.

2015;66(5):1437-1452.
3. Steffens B, Rasmussen A. The physiology of adventitious roots. Plant Physiol. 2016;170(2):603-617.
4. Kim YG, Okello D, Yang S, Komakech R, Rahmat E, Kang Y. Histological assessment of regenerating plants at callus, shoot organogenesis and plantlet stages during the in vitro micropropagation of *Asparagus cochinchinensis*. Plant Cell Tiss Org Cult. 2021;144(2):421-433.
5. Ulvrova T, Vitamvas J, Cepkova PH, Eliasova K, Janovska D, Bazant V, Viehmannova I. Micropropagation of an ornamental shrub *Disanthus cercidifolius* Maxim. and assessment of genetic fidelity of regenerants using ISSR and flow cytometry. Plant Cell Tiss Org Cult. 2021;144(3):555-566.
6. Islam MA, Macdonald SE. Ecophysiological adaptations of black spruce (*Picea mariana*) and tamarack (*Larix laricina*) seedlings to flooding. Trees. 2004;18(1):35-42.
7. Xu XW, Ji J, Xu Q, Qi XH, Chen XH. Inheritance and quantitative trail loci mapping of adventitious root numbers in cucumber seedlings under waterlogging conditions. Mol Genet Genomics. 2017;292(2):353-364.
8. Strubinska J, Hanaka A. Adventitious root system reduces lead uptake and oxidative stress in sunflower seedlings. Biol Plantarum. 2011;55(4):771-774.
9. Brijwal L, Pandey A, Tamta S. In vitro propagation of the endangered species *Berberis aristata* DC. via leaf-derived callus. In Vitro Cell Dev-Pl. 2015;51(6):637-647.
10. Wojtania A, Skrzypek E, Marasek-Ciolakowska A. Soluble sugar, starch and phenolic status during rooting of easy- and difficult-to-root magnolia cultivars. Plant Cell Tiss Org Cult. 2019;136(3):499-510.
11. Lerin J, Ribeiro YRD, de Oliveira TD, Silveira V, Santa-Catarina C. Histomorphology and proteomics during rooting of in vitro shoots in *Cariniana legalis* (Lecythidaceae), a difficult-to-root endangered species from the Brazilian Atlantic Forest. Plant Cell Tiss Org Cult. 2021;144(2):325-344.
12. Liang Y, Bai X, Xu X, Xu H, Wang J, Pan P. Direct in vitro organogenesis from sprouted seeds of a highly economical and ecological valued tree, Korean pine. Plant Cell Tiss Org Cult. 2021;148,197-207.
13. Yang LL, Chao LQ, Su XH, Wang CY, Dong CM, Chen SQ. High-frequency in vitro plantlet regeneration in *Lilium davidii var. unicolour* Salisb, an important edible and medicinal plant, and confirmation of genetic fidelity of regeneration plantlets using ISSR markers. Plant Biotechnol Rep. 2021;15(4):435-446.
14. Nameth MB, Goron TL, Dinka SJ, Morris AD, English J, Lewis D, Oro R, Raizada MN. The initial hours of post-excision light are critical for adventitious root regeneration from *Arabidopsis thaliana* (L.) Heynh. cotyledon explants. In Vitro Cell Dev-Pl. 2018;54(3):273-290.
15. Brondani GE, Baccarin FJB, de Wit Ondas HW, Stape JL, Gonçalves AN, Almeida Md. Low temperature, IBA concentrations and optimal time for adventitious rooting of *Eucalyptus benthamii* mini-cuttings. J Forestry Res. 2012;23(4):583-592.

16. Kim HJ, Lynch JP, Brown KM. Ethylene insensitivity impedes a subset of responses to phosphorus deficiency in tomato and petunia. Plant Cell Environ. 2008;31(12):1744-1755.
17. Wang HZ, Pak S, Yang J, Wu Y, Li WL, Feng H, Yang JL, Wei HR, Li CH. Two high hierarchical regulators, PuMYB40 and PuWRKY75, control the low phosphorus driven adventitious root formation in *Populus ussuriensis*. Plant Biotechnol J. 2022;20(8):1561-1577.
18. Zhao S, Zhao XW, Xu XF, Han ZH, Qiu CP. Transcription factor IAA27 positively regulates P uptake through promoted adventitious root development in apple plants. Int J Mol Sci. 2022;23(22):14029.
19. Schwambach J, Fadanelli C, Fett-Neto AG. Mineral nutrition and adventitious rooting in microcuttings of *Eucalyptus globulus*. Tree Physiol. 2005;25(4):487-494.
20. Haque SM, Ghosh B. A submerged culture system for rapid micropropagation of the commercially important aquarium plant, "Amazon sword' (*Echinodorus* "Indian Red'). In Vitro Cell Dev-Pl. 2019;55(1):81-87.
21. Haque SM, Ghosh B. Productive method for commercial propagation through direct embryogenesis and organogenesis in *Ledebouria revoluta*-an underutilized medicinal plant with cardioprotective properties. Ind Crop Prod. 2020;157:112941.
22. Lloyd GB, McCown BH. Commercially feasible micropropagation of mountain laurel, *Kalmia latifolia*, by use of shoot-tip culture. Proc Int Plant Prop Soc. 1980;30:421–427.
23. Khan MI, Ahmad N, Anis M. The role of cytokinins on in vitro shoot production in *Salix tetrasperma* Roxb.: a tree of ecological importance. Trees. 2011;25(4):577-584.
24. Zhang W, Fan J, Tan Q, Zhao M, Cao F. Mechanisms underlying the regulation of root Formation in *Malus hupehensis* stem cuttings by using exogenous hormones. J Plant Growth Regul. 2017;36(1):174-185.
25. An HS, Zhang JY, Xu FJ, Jiang S, Zhang XY. Transcriptomic profiling and discovery of key genes involved in adventitious root formation from green cuttings of highbush blueberry (*Vaccinium corymbosum* L.). BMC Plant Biol. 2020;20(1).
26. Li K, Tian HY, Mao JP, Khan A, Tahir MM, Li SH, Chen SY, Shao Y, Zhang D. Effect of darkness treatment on the morphology, hormone status and gene expression of developing adventitious root in apple rootstock. Plant Cell Tiss Org cult. 2022;148:331-346.
27. Stevens ME, Woeste KE, Pijut PM. Localized gene expression changes during adventitious root formation in black walnut (*Juglans nigra* L.). Tree Physiol. 2018;38(6):877-894.
28. Zhai S, Cai W, Xiang ZX, Chen CY, Lu YT, Yuan TT. PIN3-mediated auxin transport contributes to blue light-induced adventitious root formation in *Arabidopsis*. Plant Sci. 2021;312:111044.
29. Qi XH, Li QQ, Ma XT, Qian CL, Wang HH, Ren NN, Shen CX, Huang SM, Xu XW, Xu Q, et al. Waterlogging-induced adventitious root formation in cucumber is regulated by ethylene and auxin through reactive oxygen species signalling. Plant Cell Environ. 2019;42(5):1458-1470.
30. Tao GY, Xie YH, Li WF, Li KP, Sun C, Wang HM, Sun XM. LkARF7 and LkARF19 overexpression promote adventitious root formation in a heterologous poplar model by positively regulating *LkBBM1*. Commun Biol. 2023;6(1):372.

31. Li YH, Zhang HN, Wu QS, Muday GK. Transcriptional sequencing and analysis of major genes involved in the adventitious root formation of mango cotyledon segments. Planta. 2017;245(6):1193-1213.
32. Wang YP, Zhao HL, Hu XH, Zhang Y, Zhang ZC, Zhang L, Li LX, Hou LP, Li ML. Transcriptome and hormone analyses reveal that melatonin promotes adventitious rooting in shaded cucumber hypocotyls. Front Plant Sci. 2022;13:1059482.
33. Chen KM, Guo B, Yu CM, Chen P, Chen JK, Gao G, Wang XF, Zhu AG. Comparative transcriptome analysis provides new insights into the molecular regulatory mechanism of adventitious root formation in Ramie (*Boehmeria nivea* L.). Plants. 2021;10(1):160.
34. Cheng L, Zhao M, Hu Z, Liu H, Li S. Comparative transcriptome analysis revealed the cooperative regulation of sucrose and IAA on adventitious root formation in lotus (*Nelumbo nucifera* Gaertn). BMC Genomics. 2020;21(1):653.
35. Zhang Y, Xiao ZA, Zhan C, Liu MF, Xia WX, Wang N. Comprehensive analysis of dynamic gene expression and investigation of the roles of hydrogen peroxide during adventitious rooting in poplar. BMC Plant Biol. 2019;19(1):99.
36. Fu H, Wei X, Chen Q, Yong SY, Liu QJ, Dang JB, Wu D, Liang GL, Guo QG. Comparative transcriptome analysis of molecular mechanisms underlying adventitious root developments in Huangshan Bitter tea (*Camellia gymnogyna* Chang) under red light quality. Front Plant Sci. 2023;14:1154169.
37. Chu KL, Cooper WS. An ecological reconnaissance in the native home of *Metasequoia glyptostroboides*. Ecology. 1950;31(2):260-278.
38. Tang CQ, Yang Y, Ohsawa M, Momohara A, Hara M, Cheng S, Fan S. Population structure of relict *Metasequoia glyptostroboides* and its habitat fragmentation and degradation in south-central China. Biol Conserv. 2011;144(1):279-289.
39. Ma J. A worldwide survey of cultivated *Metasequoia glyptostroboides* Hu & Cheng (Taxodiaceae: Cupressaceae) from 1947 to 2007. B Peabody Mus Nat His. 2007;48(2):235-253.
40. Juvik OJ, Nguyen XHT, Andersen HL, Fossen T. Growing with dinosaurs: natural products from the Cretaceous relict *Metasequoia glyptostroboides* Hu & Cheng-a molecular reservoir from the ancient world with potential in modern medicine. Phytochem Rev. 2016;15(2):161-195.
41. Bajpai VK, Yoon JI, Kang SC. Antioxidant and antidermatophytic activities of essential oil and extracts of *Metasequoia glyptostroboides* Miki ex Hu. Food Chem Toxicol. 2009;47(6):1355-1361.
42. Bajpai VK, Na M, Kang SC. The role of bioactive substances in controlling foodborne pathogens derived from *Metasequoia glyptostroboides* Miki ex Hu. Food Chem Toxicol. 2010;48(7):1945-1949.
43. Lee H, Oh C, Kim S, Dey DK, Kim HK, Bajpai VK, Han YK, Huh YS. *Metasequoia glyptostroboides* potentiates anticancer effect against cervical cancer via intrinsic apoptosis pathway. Sci Rep. 2021;11(1):894.
44. Yeo JY, Lee SL, Ko MS, Lee CH, Choi JY, Hwang KW, Park SY. Anti-amyloidogenic effects of *Metasequoia glyptostroboides* fruits and its active constituents. Molecules. 2023;28(3):1017.
45. Fu L, Jin J: Red list of endangered plants in China. Beijing: Science Press; 1992.

46. Farjon A. *Metasequoia glyptostroboides*. The IUCN Red List of Threatened Species. 2013.
47. Zhao Y, Thammannagowda S, Staton M, Tang S, Xia X, Yin W, Liang H. An EST dataset for *Metasequoia glyptostroboides* buds: the first EST resource for molecular genomics studies in Metasequoia. Planta. 2012;237(3):755-770.
48. Xiong Y, Chen S, Guo B, Niu M, Zhang X, Li Y, Wu K, Zheng F, da Silva JAT, Zeng S *et al*. An efficient micropropagation protocol for *Metasequoia glyptostroboides* Hu et Cheng from shoot segments of 2-year-old trees. Trees. 2019;34(1):307-313.
49. Diaz Sala C. A perspective on adventitious root formation in tree species. Plants. 2020;9(12).
50. Vielba JM, Rico S, Sevgin N, Castro-Camba R, Covelo P, Vidal N, Sanchez C. Transcriptomics analysis reveals a putative role for hormone signaling and MADS-Box genes in mature chestnut shoots rooting recalcitrance. Plants. 2022;11(24):3486.
51. Regni L, Facchin SL, da Silva DF, De Cesaris M, Famiani F, Proietti P, Micheli M. Neem oil to reduce zeatin use and optimize the rooting phase in *Olea europaea* L. micropropagation. Plants. 2023;12(3):576.
52. El Banna MF, Farag NBB, Massoud HY, Kasem MM. Exogenous IBA stimulated adventitious root formation of *Zanthoxylum beecheyanum* K. Koch stem cutting: Histo-physiological and phytohormonal investigation. Plant Physiol Biochem. 2023;197:107639.
53. Liu X, Sun L, Nie T, Chen Y, Yin Z. *In vitro* rapid propagation technology system of *Dendrobium moniliforme* (L.) Sw., a threatened orchid species in China. Plant Biotechnol Rep. 2023;17(3):369-378.
54. Gang R, Komakech R, Chung Y, Okello D, Kim WJ, Moon BC, Yim N-H, Kang Y. *In vitro* propagation of *Codonopsis pilosula* (Franch.) Nannf. using apical shoot segments and phytochemical assessments of the maternal and regenerated plants. BMC Plant Biol. 2023;23(1):33.
55. Guo JY, Chen GD, Zhang XZ, Li TX, Yu HY, Liu CJ. Quantitative trait locus analysis of adventitious and lateral root morphology of barley grown at low and high P. Funct Plant Biol. 2018;45(9):957-967.
56. Negi M, Sanagala R, Rai V, Jain A. Deciphering phosphate deficiency-mediated temporal effects on different root traits in rice grown in a modified hydroponic system. Front Plant Sci. 2016;7:550.
57. Pan R, Liu Y, Buitrago S, Jiang W, Gao HR, Han H, Wu C, Wang YL, Zhang WY, Yang XS. Adventitious root formation is dynamically regulated by various hormones in leaf-vegetable sweetpotato cuttings. J Plant Physiol. 2020;253:153267.
58. Otiende MA, Fricke K, Nyabundi JO, Ngamau K, Hajirezaei MR, Druege U. Involvement of the auxin-cytokinin homeostasis in adventitious root formation of rose cuttings as affected by their nodal position in the stock plant. Planta. 2021;254(4):65.
59. Olatunji D, Geelen D, Verstraeten I. Control of endogenous auxin levels in plant root development. Int J Mol Sci. 2017;18(12):2587.
60. Chen LQ, Tong JH, Xiao LT, Ruan Y, Liu JC, Zeng MH, Huang H, Wang JW, Xu L. YUCCA-mediated auxin biogenesis is required for cell fate transition occurring during de novo root organogenesis in *Arabidopsis*. J Exp Bot. 2016;67(14):4273-4284.

61. Zhao D, Wang YT, Feng C, Wei Y, Peng X, Guo X, Guo XW, Zhai ZF, Li J, Shen XS, et al. Overexpression of *MsGH3.5* inhibits shoot and root development through the auxin and cytokinin pathways in apple plants. Plant J. 2020;103(1):166-183.
62. Gutierrez L, Mongelard G, Flokova K, Pacurar DI, Novak O, Staswick P, Kowalczyk M, Pacurar M, Demailly H, Geiss G, et al. Auxin controls *Arabidopsis* adventitious root initiation by regulating jasmonic acid homeostasis. Plant Cell. 2012;24(6):2515-2527.
63. da Costa CT, de Almeida MR, Ruedell CM, Schwambach J, Maraschin FS, Fett-Neto AG. When stress and development go hand in hand: main hormonal controls of adventitious rooting in cuttings. Front Plant Sci. 2013;4:133.
64. Druege U, Hilo A, Pérez-Pérez JM, Klopotek Y, Acosta M, Shahinnia F, Zerche S, Franken P, Hajirezaei MR. Molecular and physiological control of adventitious rooting in cuttings: phytohormone action meets resource allocation. Ann Bot. 2019;123(6):929-949.
65. Wang YX, Pang DD, Ruan L, Liang JB, Zhang Q, Qian YH, Zhang YZ, Bai PX, Wu LY, Cheng H, et al. Integrated transcriptome and hormonal analysis of naphthalene acetic acid-induced adventitious root formation of tea cuttings (*Camellia sinensis*). BMC Plant Biol. 2022;22(1):319.
66. Alallaq S, Ranjan A, Brunoni F, Novak O, Lakehal A, Bellini C. Red light controls adventitious root regeneration by modulating hormone homeostasis in *Picea abies* seedlings. Front Plant Sci. 2020;11:586140.
67. Niu SH, Li ZX, Yuan HW, Fang P, Chen XY, Li W. Proper gibberellin localization in vascular tissue is required to regulate adventitious root development in tobacco. J Exp Bot. 2013;64(11):3411-3424.
68. Li SW, Shi RF, Leng Y, Zhou Y. Transcriptomic analysis reveals the gene expression profile that specifically responds to IBA during adventitious rooting in mung bean seedlings. BMC Genomics. 2016;17:43.
69. Li K, Liang YQ, Xing LB, Mao JP, Liu Z, Dong F, Meng Y, Han MY, Zhao CP, Bao L, et al. Transcriptome analysis reveals multiple hormones, wounding and sugar signaling pathways mediate adventitious root formation in apple rootstock. Int J Mol Sci. 2018;19(8):2201.
70. Li AM, Lakshmanan P, He WZ, Tan HW, Liu LM, Liu HJ, Liu JX, Huang DL, Chen ZL. Transcriptome profiling provides molecular insights into auxin-induced adventitious root formation in sugarcane (*Saccharum* spp. interspecific hybrids) microshoots. Plants. 2020;9(8):931.
71. Brunoni F, Collani S, Casanova-Saez R, Simura J, Karady M, Schmid M, Ljung K, Bellini C. Conifers exhibit a characteristic inactivation of auxin to maintain tissue homeostasis. New Phytol. 2020;226(6):1753-1765.
72. Dong CJ, Liu XY, Xie LL, Wang LL, Shang QM. Salicylic acid regulates adventitious root formation via competitive inhibition of the auxin conjugation enzyme CsGH3.5 in cucumber hypocotyls. Planta. 2020;252(5).
73. Jiang LJ, Zhang DH, Liu C, Shen WY, He JQ, Yue QY, Niu CD, Yang F, Li XW, Shen XX, et al. MdGH3.6 is targeted by MdMYB94 and plays a negative role in apple water-deficit stress tolerance. Plant J. 2022;109(5):1271-1289.

74. Salehin M, Bagchi R, Estelle M. SCFTIR1/AFB-based auxin perception: Mechanism and role in plant growth and development. Plant Cell. 2015;27(1):9-19.
75. Lakehal A, Chaabouni S, Cavel E, Le Hir R, Ranjan A, Raneshan Z, Novak O, Pacurar DI, Perrone I, Jobert F, et al. A molecular framework for the control of adventitious rooting by TIR1/AFB2-Aux/IAA-dependent auxin signaling in *Arabidopsis*. Mol Plant. 2019;12(11):1499-1514.
76. Shu WB, Zhou HJ, Jiang C, Zhao ST, Wang LQ, Li QZ, Yang ZQ, Groover A, Lu MZ. The auxin receptor TIR1 homolog (PagFBL 1) regulates adventitious rooting through interactions with Aux/IAA28 in Populus. Plant Biotechnol J. 2019;17(2):338-349.
77. Ren H, Gray WM. SAUR proteins as effectors of hormonal and environmental signals in plant growth. Mol Plant. 2015;8(8):1153-1164.
78. Kant S, Bi YM, Zhu T, Rothstein SJ. *SAUR39*, a small auxin-up RNA gene, acts as a negative regulator of auxin synthesis and transport in rice. Plant Physiol. 2009;151(2):691-701.
79. Kong YY, Zhu YB, Gao C, She WJ, Lin WQ, Chen Y, Han N, Bian HW, Zhu MY, Wang JH. Tissue-specific expression of SMALL AUXIN UP RNA41 differentially regulates cell expansion and root meristem patterning in *Arabidopsis*. Plant Cell Physiol. 2013;54(4):609-621.
80. Yin HJ, Li MZ, Lv MH, Hepworth SR, Li DD, Ma CF, Li J, Wang SM. SAUR15 promotes lateral and adventitious root development via activating H^+-ATPases and auxin biosynthesis. Plant Physiol. 2020;184(2):837-851.
81. Yang Y, Miao Y, Zhong S, Fang Q, Wang Y, Dong B, Zhao H. Genome-wide identification and expression analysis of *XTH* gene family during flower-opening stages in *Osmanthus fragrans*. Plants. 2022;11(8):081015.
82. Li YH, Hua J, Hou XM, Qi NA, Li CX, Wang CL, Yao YD, Huang DJ, Zhang HS, Liao WB. Brassinosteroids is involved in methane-induced adventitious root formation via inducing cell wall relaxation in marigold. BMC Plant Biol. 2023;23(1):2.
83. Wang ZQ, Hua JF, Yin YL, Gu CS, Yu CG, Shi Q, Guo JB, Xuan L, Yu FY. An integrated transcriptome and proteome analysis reveals putative regulators of adventitious root formation in *Taxodium* "Zhongshanshan". Int J Mol Sci. 2019;20(5):1225.
84. Li S, Tahir MM, Wu T, Xie L, Zhang X, Mao J, Ayyoub A, Xing L, Zhang D, Shao Y. Transcriptome analysis reveals multiple genes and complex hormonal-mediated interactions with PEG during adventitious root formation in apple. Int J Mol Sci. 2022;23(2):976.
85. Correa LR, Stein RJ, Fett-Neto AG. Adventitious rooting of detached *Arabidopsis thaliana* leaves. Biol Plant. 2012;56(1):25-30.
86. Du J, Wang S, He C, Zhou B, Ruan YL, Shou H. Identification of regulatory networks and hub genes controlling soybean seed set and size using RNA sequencing analysis. J Exp Bot. 2017;68(8):1955-1972.
87. He KH, Zhao Z, Ren W, Chen Z, Chen LM, Chen FJ, Mi GH, Pan QC, Yuan LX. Mining genes regulating root system architecture in maize based on data integration analysis. Theor Appl Genet. 2023;136(6):127.

88. Li KQ, Wang J, Kuang LQ, Tian Z, Wang XF, Dun XL, Tu JX, Wang HZ. Genome-wide association study and transcriptome analysis reveal key genes affecting root growth dynamics in rapeseed. Biotech Biofuels. 2021;14(1):178.
89. Chen SF, Zhou YQ, Chen YR, Gu J. fastp: an ultra-fast all-in-one FASTQ preprocessor. Bioinformatics. 2018;34(17):884-890.
90. Fu F, Song C, Wen C, Yang L, Guo Y, Yang X, Shu Z, Li X, Feng Y, Liu B, et al. The Metasequoia genome and evolutionary relationship among redwoods. Plant Commun. 2023:100643.
91. Kim D, Landmead B, Salzberg SL. HISAT: a fast spliced aligner with low memory requirements. Nat Methods. 2015;12(4):357-U121.
92. Pertea M, Pertea GM, Antonescu CM, Chang TC, Mendell JT, Salzberg SL. StringTie enables improved reconstruction of a transcriptome from RNA-seq reads. Nat Biotechnol. 2015;33(3):290-295.
93. Li B, Dewey CN. RSEM: accurate transcript quantification from RNA-Seq data with or without a reference genome. BMC Bioinformatics. 2011;12:323.
94. Love MI, Huber W, Anders S. Moderated estimation of fold change and dispersion for RNA-seq data with DESeq2. Genome Biol. 2014;15(12):550.
95. Xie C, Mao XZ, Huang JJ, Ding Y, Wu JM, Dong S, Kong L, Gao G, Li CY, Wei LP. KOBAS 2.0: a web server for annotation and identification of enriched pathways and diseases. Nucl Acids Res. 2011;39:316-322.
96. Langfelder P, Horvath S. WGCNA: an R package for weighted correlation network analysis. BMC Bioinformatics. 2008;9:559.
97. Livak KJ, Schmittgen TD. Analysis of relative gene expression data using real-time quantitative PCR and the $2^{-\Delta\Delta CT}$ method. Methods. 2001;25(4):402-408.

Tables

Tables 1-2 are available in the Supplementary Files section.

Figures

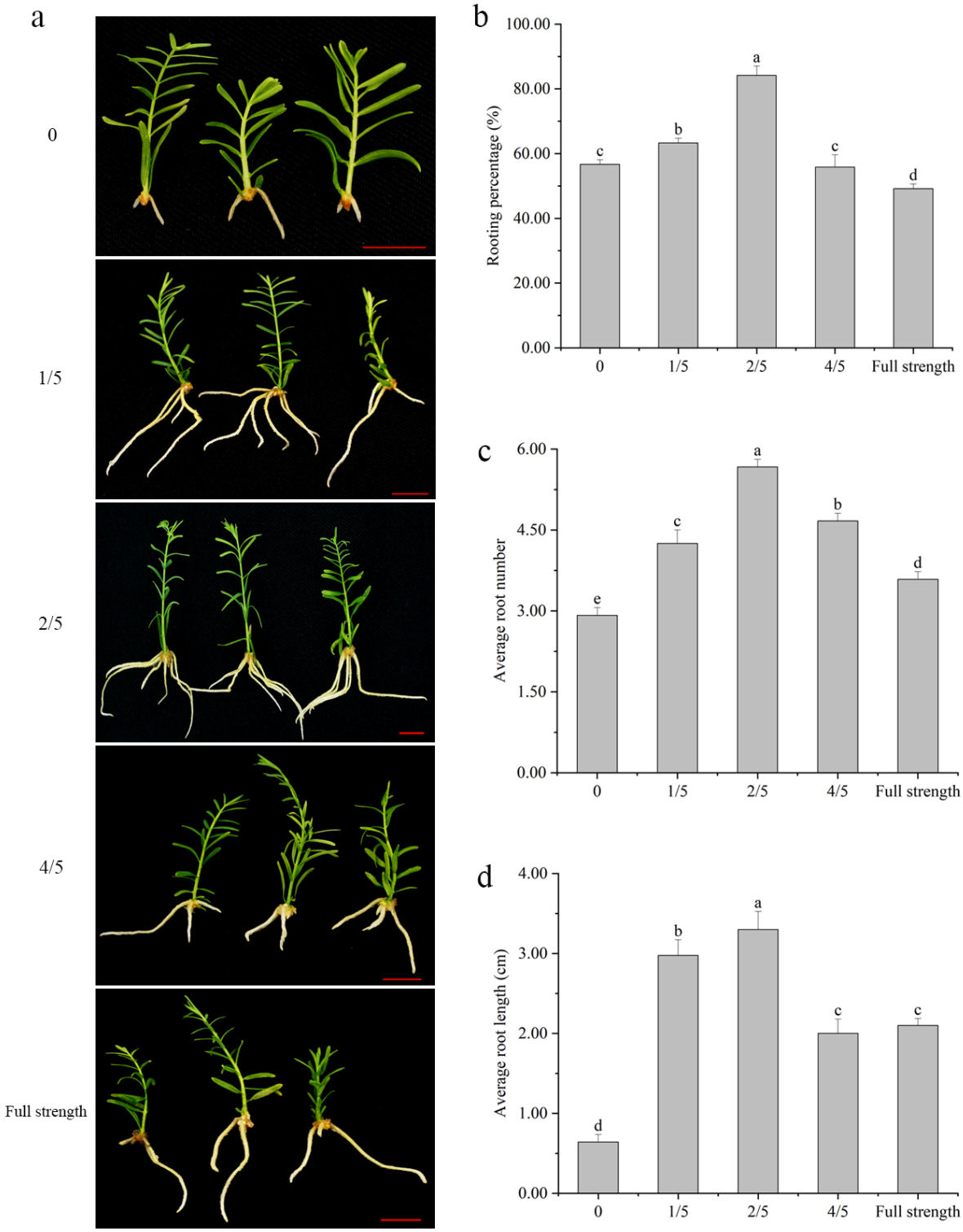


Figure 1

Adventitious root induction of *Metasequoia glyptostroboides* shoots during *in vitro* rooting after 30 d (a, phenotype of adventitious rooting in different strength of WPM medium; b, rooting percentage; c, average root number; d, average root length) treatment. Red bars = 1 cm. Treatments (X-axis) indicate the strength of WPM medium. Bars indicatemeans ± SD. Different letters indicate statistically significant differences between the groups based on Duncan's multiple range test ($p < 0.05$) for the designated

treatments. Forty shoots were prepared for each treatment, and three replicates were performed for each treatment. Graph was generated by OriginPro 2021.

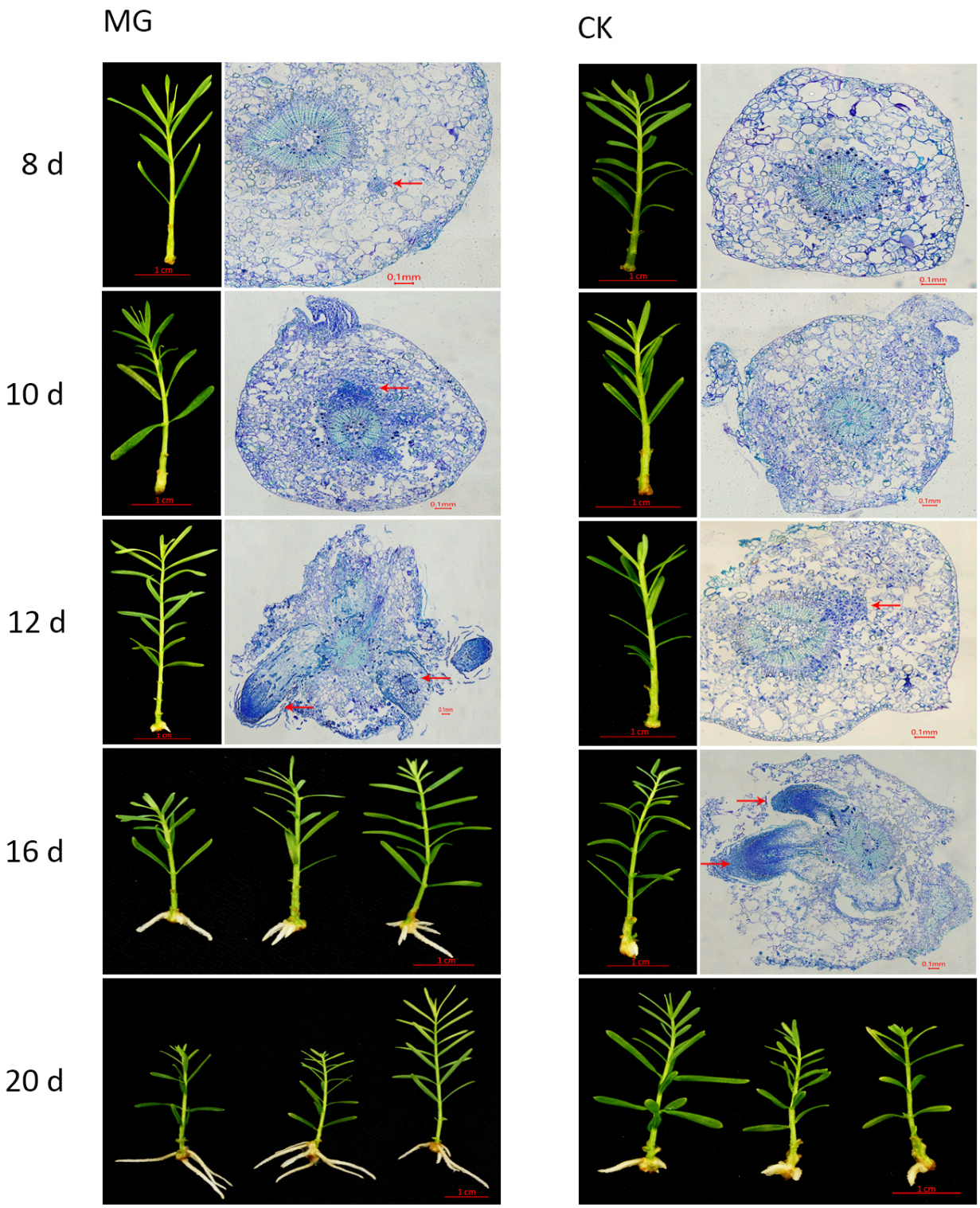


Figure 2

Adventitious root development of *Metasequoia glyptostroboides* shoots stem base (0.5-1.0 cm) after 8, 10, 12, 16 and 20 d in 2/5 (MG) and full-strength (CK) WPM treatment during *in vitro* rooting. Red bars in photos representing phenotypic changes = 1 cm. Red bars in photos of histological analyses = 0.1 mm.

Red arrows indicate meristematic cells (8 d in MG), the root primordium (10 d in MG; 12 d in CK), and adventitious roots (12 d in MG; 16 d in CK).

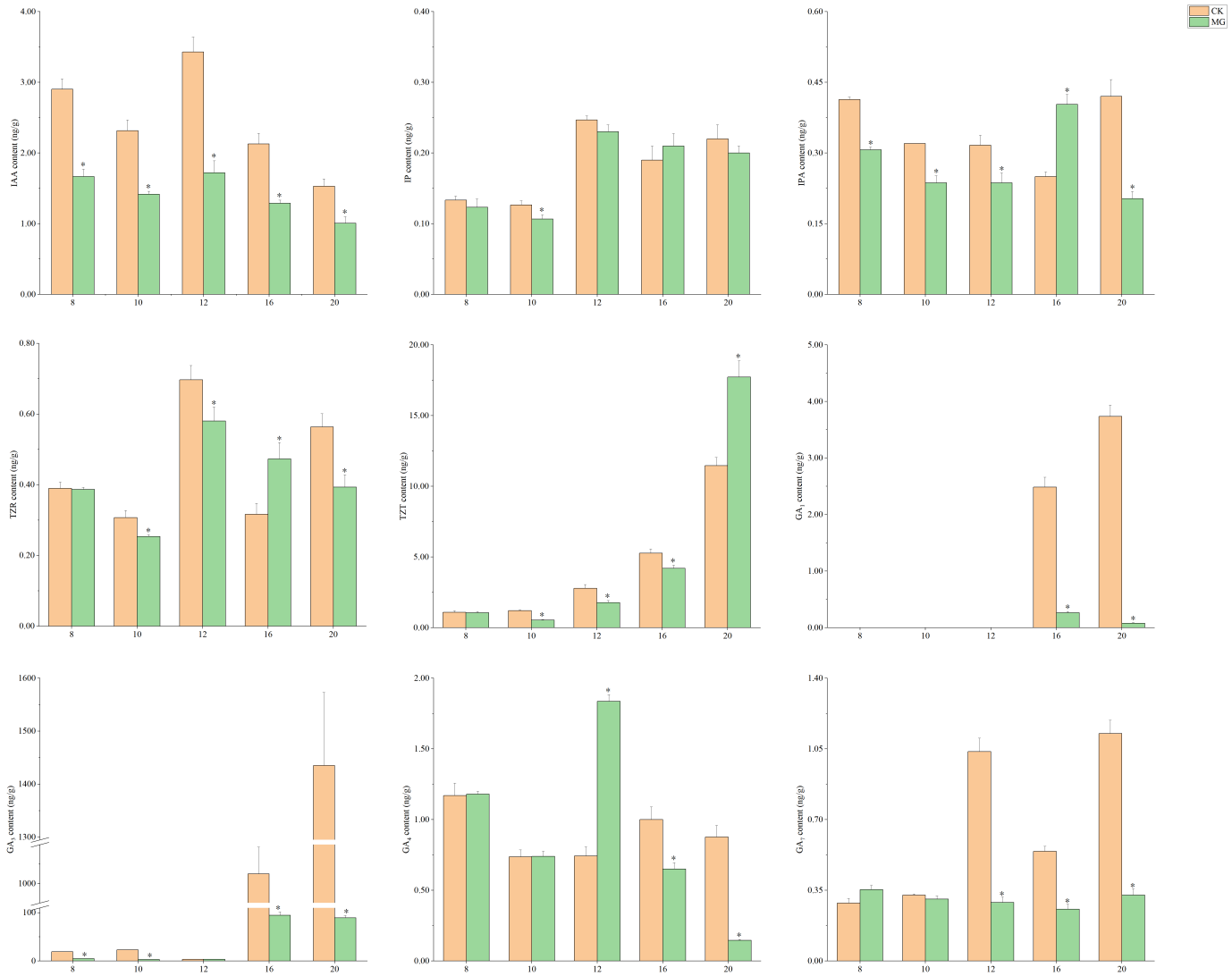


Figure 3

Determination of endogenous IAA, IP, IPA, TZT, TZR, GA_1, GA_3, GA_4 and GA_7 content at 8, 10, 12, 16, and 20 d in 2/5 (MG) and full-strength (CK) WPM treatment in stem bases of *Metasequoia glyptostroboides*. Bars indicate means±SD. Asterisk indicates significant differences following one-way ANOVA and according to the Mann Whitney non-parametric test ($p < 0.05$) in comparisons of MG with CK at designed time points. Graph was generated by OriginPro 2021. The green color indicated MG group, and the orange color indicate CK group.

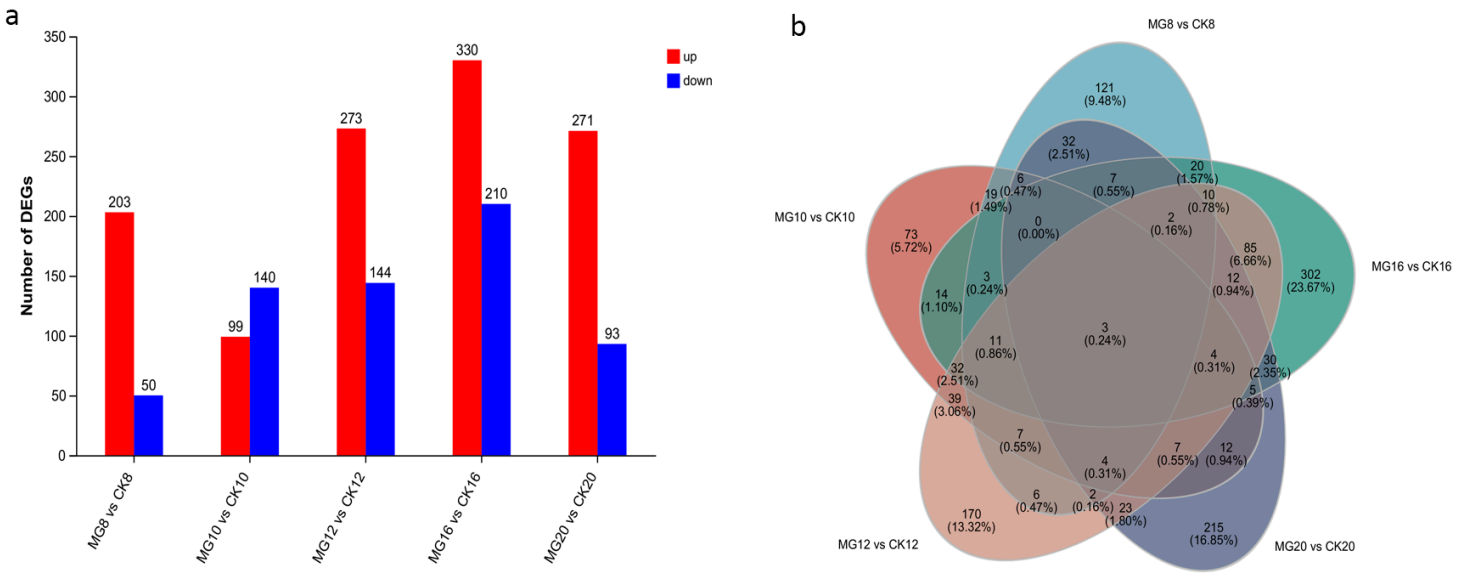


Figure 4

DEGs identified in different comparisons during adventitious root development of *Metasequoia glyptostroboides*. (a) Number of up- and down-regulated DEGs at 8, 10, 12, 16 and 20 d compared 2/5-strength WPM treatment (MG) with the control (CK). The X-axis represents the groups that were compared during rooting, while the Y-axis represents the number of DEGs. (b) Venn diagram of DEGs (absolute numbers and relative percentage values in parentheses below) between different comparisons.

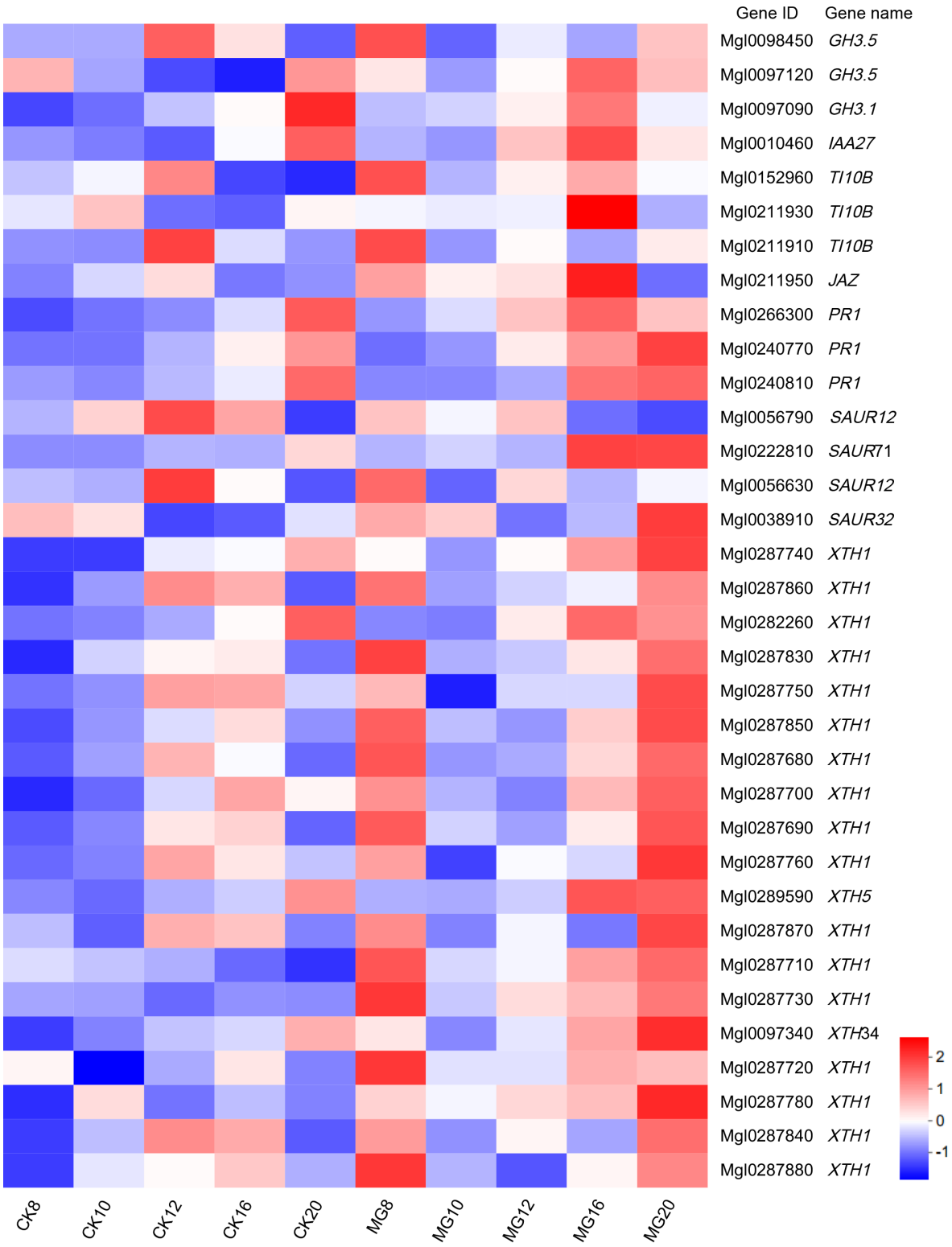


Figure 5

Expression analysis of DEGs enriched in the “plant hormone signal transduction” pathway. Different colors indicate DEG expression levels based on log10 (FPKM) values. Blue represents down-regulated expression while red represents up-regulated expression.

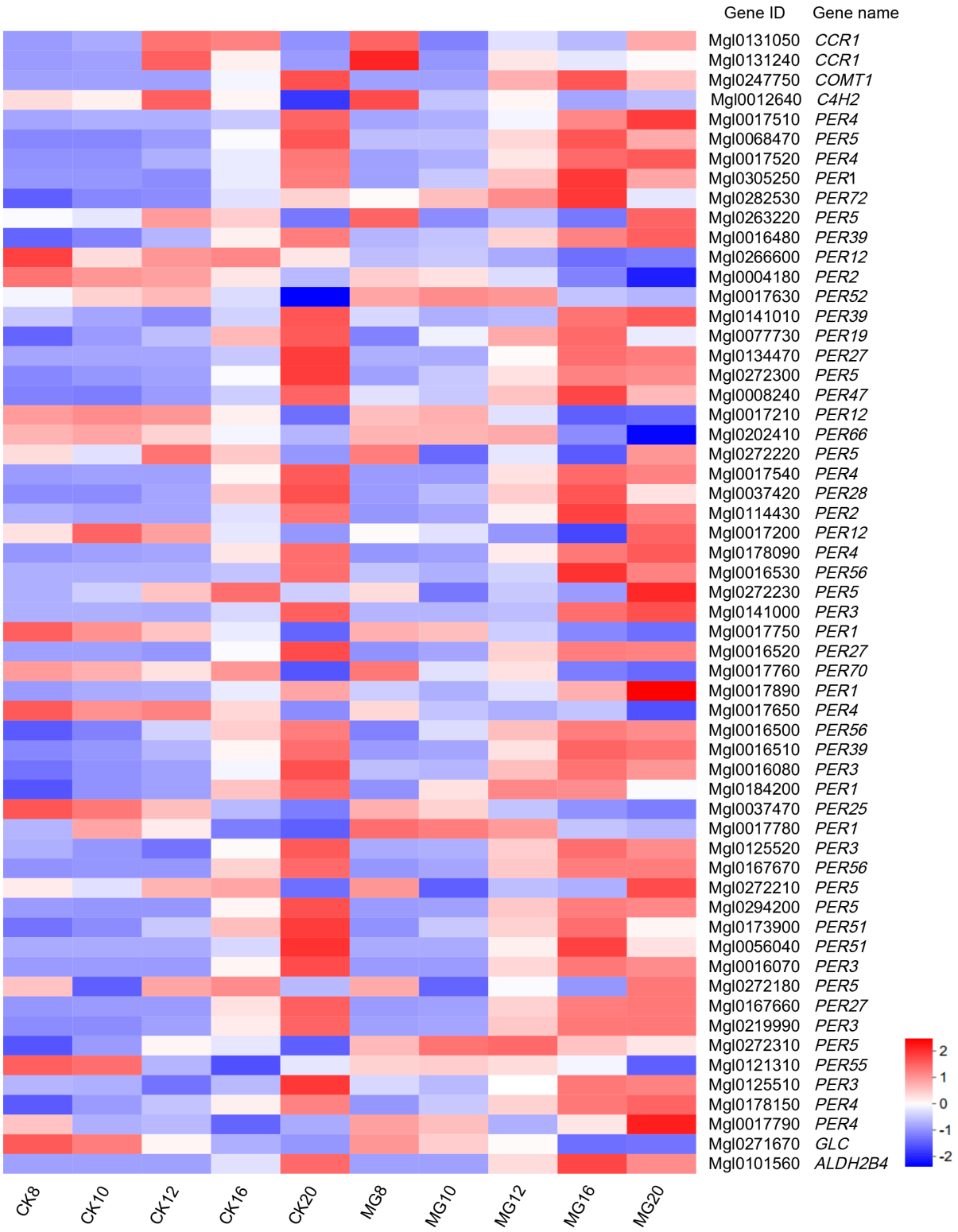


Figure 6

Expression analysis of DEGs enriched in the “phenylpropanoid biosynthesis” pathway. Different colors indicate DEG expression levels based on log10 (FPKM) values. Blue represents down-regulated expression while red represents up-regulated expression.

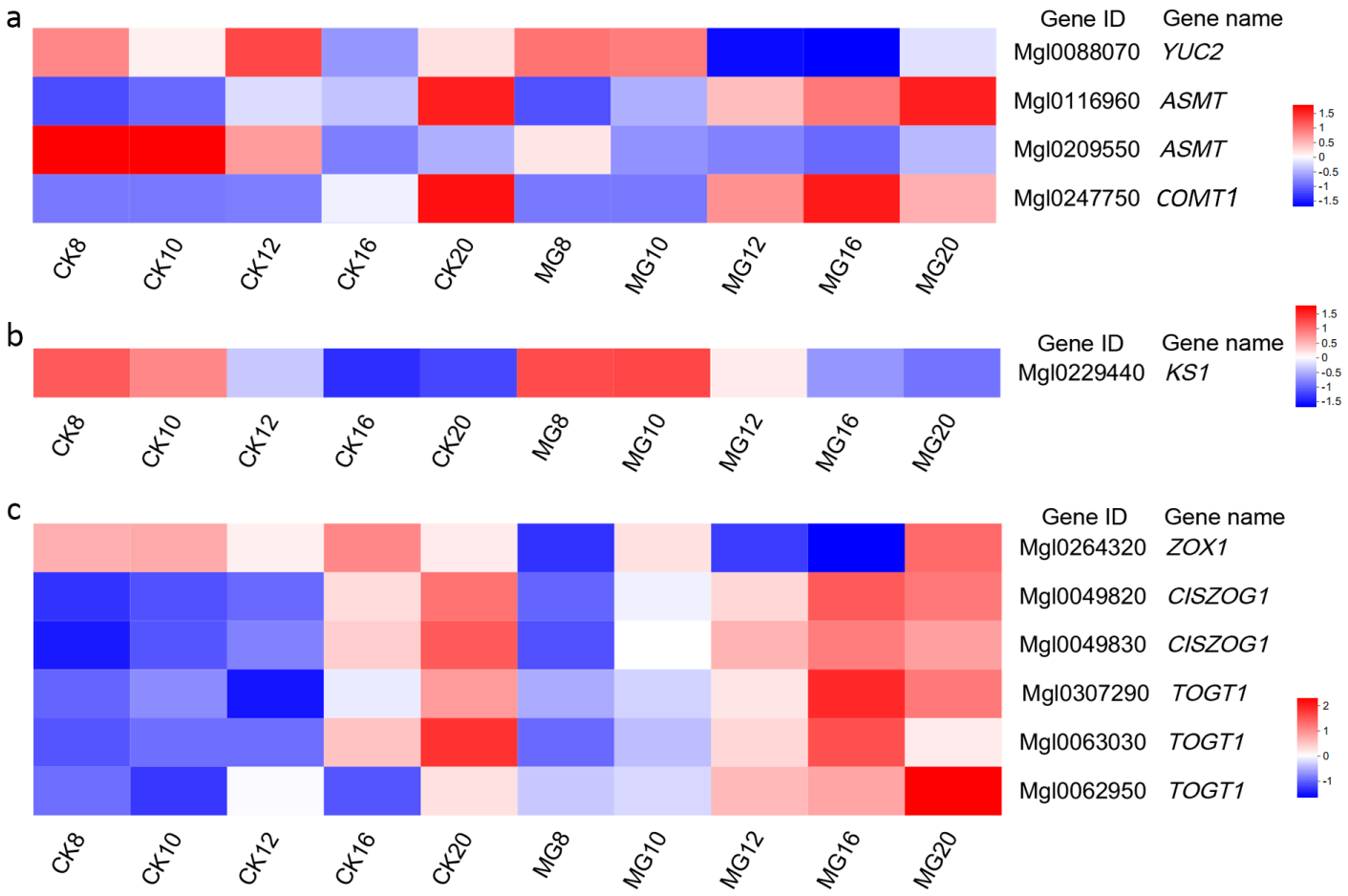


Figure 7

Expression analysis of DEGs enriched in “tryptophan metabolism” (a), “diterpenoid biosynthesis” (b) and “zeatin biosynthesis” (c) pathways. Different colors indicate DEG expression levels based on log10 (FPKM) values. Blue represents down-regulated expression whilered represents up-regulated expression.

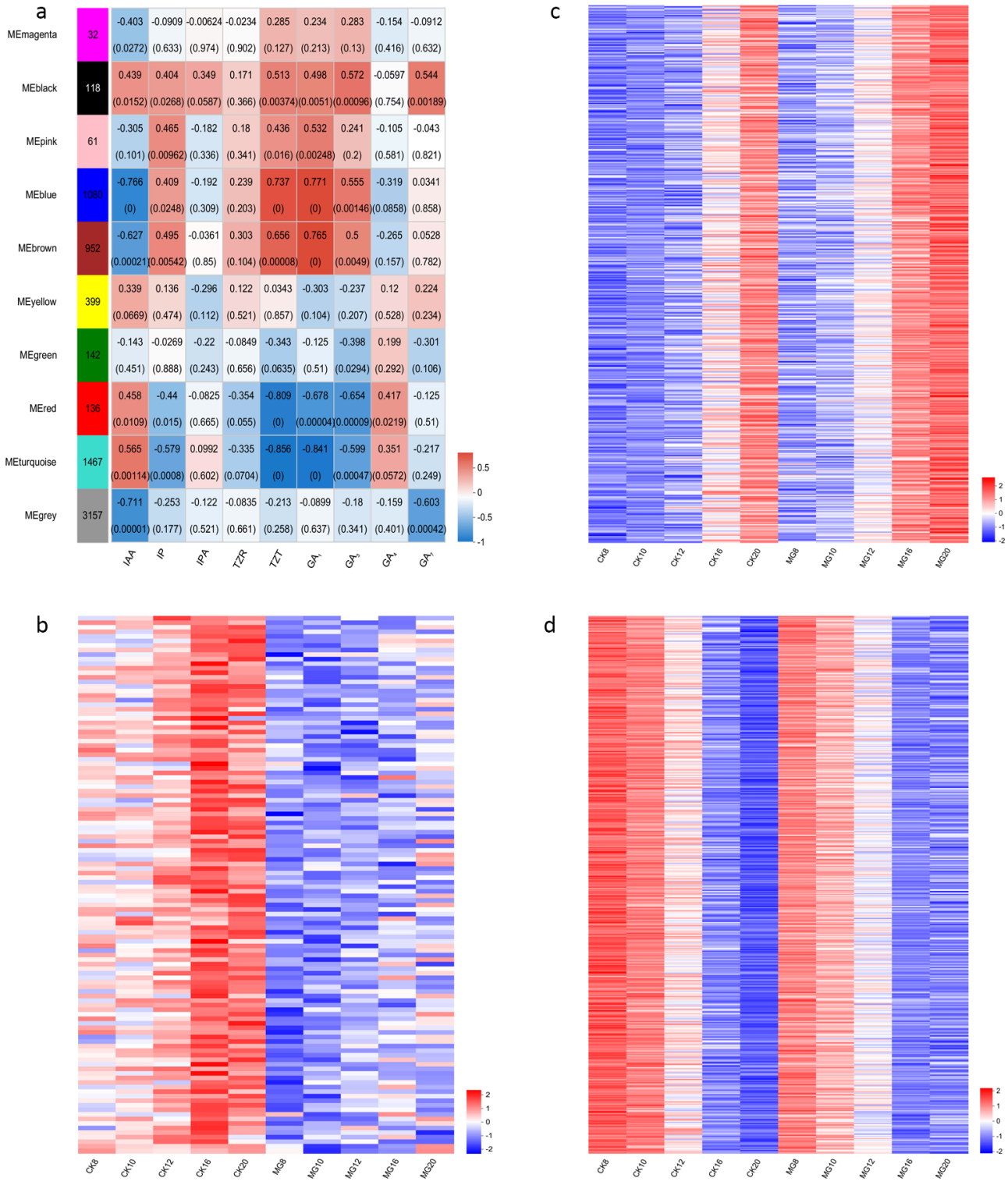


Figure 8

WGCNA-based co-expression analysis of genes in AR formation of *Metasequoia glyptostroboides* stems. (a) Correlation analysis was carried out between the co-expression modules of genes and endogenous hormone content. The numbers in the column on the left indicate the number of genes in eachmodule, and each set of data on the right indicates the correlation coefficient and significance *p*-value of the module with the phenotype (in parentheses). (b-d) Heatmaps of top 500 connectivity genes

corresponding to the MEblack, MEblue and MEturquoise modules,respectively. The different colors indicate DEG expression levels based on log10 (FPKM) values. Blue represents down-regulated expression while red represents up-regulated expression.

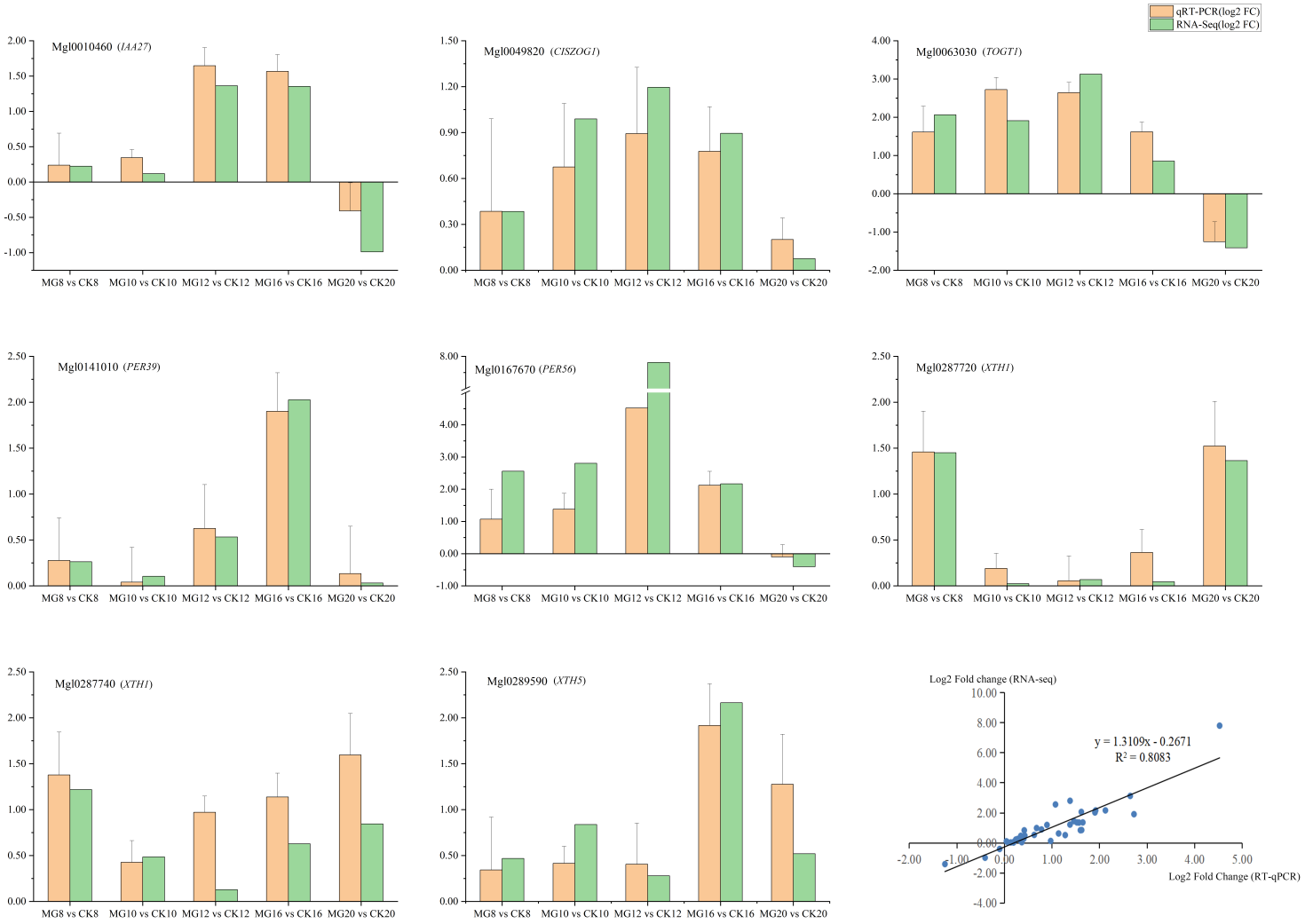


Figure 9

Analysis of the fold changes of eight candidate genes expressed in *Metasequoia glyptostroboides* stems during adventitious root induction and formation, determined by RNA-seq (green) and RT-qPCR (orange). Bars indicatemeans ± SD. The X-axis represents the time point after each treatment while the Y-axis represents the log2 (fold change). In correlations analysis of the expression levels of the DEGs measured via RNA-seq and RT-qPCR, the X-axis represents log2 (fold change) in RT-qPCR and the Y-axis represents log2 (fold change) in RNA-seq.Graph was generated by OriginPro 2021.

Image not available with this version

Figure 10

A possible network of AR-promoting potential of 2/5-strength WPM for *Metasequoia glyptostroboides*. Red arrows indicated up-regulated DEGs, and blue arrows indicated down-regulated DEGs. Green arrows indicated an interaction between the corresponding pathway. Orange arrows indicated the decrease in hormone accumulation. The complex interactions between hormones biosynthesis and the expression of genes related to plant hormone signal transduction and phenylpropanoid biosynthesis pathway contributed to the AR formation of *M. glyptostroboides* induced by 2/5-strength WPM under *in vitro* culture.

Supplementary Files

This is a list of supplementary files associated with this preprint. Click to download.

- Table1.xlsx
- Table2.xlsx
- FigureS1.pdf
- FigureS2.pdf
- TableS1.xlsx
- TableS2.xlsx
- TableS3.xlsx
- TableS4.xlsx
- TableS5.xlsx